# UNDERSTANDING MULTIMODAL LLMS UNDER DISTRIBUTION SHIFTS: AN INFORMATION-THEORETIC APPROACH

**Changdae Oh**[1], **Zhen Fang**[2], **Shawn Im**[1], **Xuefeng Du**[1], **Yixuan Li**[1]
[1]University of Wisconsin–Madison [2]University of Technology Sydney
{changdae,shawnim,xfdu,sharonli@cs.wisc.edu} zhen.fang@uts.edu.au

## ABSTRACT

Multimodal large language models (MLLMs) have shown promising capabilities but struggle under distribution shifts, where evaluation data differ from instruction tuning distributions. Although previous works have provided empirical evaluations, we argue that establishing a formal framework that can characterize and quantify the risk of MLLMs is necessary to ensure the safe and reliable application of MLLMs in the real world. By taking an information-theoretic perspective, we propose the first theoretical framework that enables the quantification of the maximum risk of MLLMs under distribution shifts. Central to our framework is the introduction of Effective Mutual Information (EMI), a principled metric that quantifies the relevance between input queries and model responses. We derive an upper bound for the EMI difference between in-distribution (ID) and out-of-distribution (OOD) data, connecting it to visual and textual distributional discrepancies. Extensive experiments on real benchmark datasets, spanning 61 shift scenarios empirically validate our theoretical insights.

## 1 INTRODUCTION

Multimodal large language models (MLLMs) have demonstrated remarkable capabilities in handling complex tasks that require reasoning over both visual and textual modalities. By leveraging visual instruction tuning Liu et al. (2023); Dai et al. (2023); Zhu et al. (2024), MLLMs have shown promise in answering open-ended questions and generating contextually relevant captions. As a critical aspect for real-world deployment, MLLMs are expected to operate robustly in the wild, where *distribution shifts* occur—that is, when the evaluation data deviates from the instruction tuning data, whether due to changes in visual inputs (e.g, domain-specific images), textual inputs (e.g., linguistic variations), or the combination thereof. However, negative reports on MLLM failures under edge cases have steadily emerged, raising concerns about their reliability.

For example, MLLMs struggle with queries in specialized domains such as medical and chemistry Zhang et al. (2024a); Han et al. (2024), perform poorly on simple classification tasks compared with open-ended question answering Zhang et al. (2024b); Zhai et al. (2024), and frequently exhibit hallucination Li et al. (2023b); Ye-Bin et al. (2025). Given the increasing impact of MLLMs, it is crucial to understand their failure modes under distribution shifts. Despite the significance of the problem, existing works often lack a fine-grained diagnosis for various factors of shifts. More importantly, the absence of a formal framework to explain the underlying principle further hinders the systematic understanding of MLLMs' behavior. This motivates us to raise the research question:

***Can we derive a theoretical framework to characterize MLLM's behavior under distribution shifts?***

To address this, we propose an information-theoretic framework that characterizes MLLM performance under distribution shifts with theoretical rigor and practical interpretability. Our framework is well-suited for analyzing instruction-tuned models, which effectively maximizes the lower bound of mutual information between input query and response. Under this framework, we introduce *effective mutual information* (EMI) as a principled measurement for evaluating the relevance between an input query and model response. Intuitively, EMI is expected to be higher when a test input query originates from the in-distribution (ID) data similar to those used during instruction tuning, compared to when

the input comes from out-of-distribution (OOD). To quantify this performance gap, we compute the difference in EMI between ID and OOD and derive an upper bound for this difference, expressed in terms of distributional discrepancies in input and output spaces (see Theorem 4.3 and 4.4). By grounding the measure in information theory, we provide the first theoretical framework to analyze and understand the impact of distribution shifts on MLLM performance.

Beyond the theoretical rigor, we further show that our framework holds practical value. In particular, we demonstrate that EMI is closely related to the widely used empirical evaluation metric for MLLMs, win rate Ouyang et al. (2022) with an LLM judge Zheng et al. (2023). The win rate commonly relies on external judge models such as GPT-4, thus it lacks mathematical guarantees due to the black-box nature of these evaluators. In contrast, EMI provides an *theory-grounded measurement* of the relevance between input queries and the output responses of the MLLM being evaluated, offering a principled metric for assessing performance under distribution shifts.

Finally, we conduct empirical validation for the theoretical framework and show that our theorems empirically hold in real-world benchmarks. Our experiments comprehensively examine 34 synthetic and 27 natural distribution shift scenarios, resulting in a total number of 61 ID-OOD evaluations for each MLLM. Results confirm strong correlations between EMI and win rate, as well as between EMI difference and its upper bounds, demonstrating the effectiveness of our framework in capturing performance gaps under diverse shifts. Our contributions can be summarized as follows:

- We propose a new framework, effective mutual information (EMI), to analyze MLLM under distribution shift, and justify the use of EMI by showing the theoretical connection between EMI and win rate.
- We derive a theoretical upper bound of MLLM's performance gap which can be characterized by shifts over multimodal input queries and output discrepancies.
- We empirically verify our theoretical statements on 61 real-world distribution shift scenarios of open-ended question-answering benchmarks with four MLLMs.

## 2 PRELIMINARY

**Random variable and distribution.** Let $\mathcal{X} = \mathcal{X}_v \times \mathcal{X}_t$ denote the input space, where $\mathcal{X}_v$ and $\mathcal{X}_t$ correspond to the visual and textual feature spaces, respectively. Similarly, let $\mathcal{Y}$ denote the response space. We define $\mathbf{X} = (X_v, X_t) \in \mathcal{X}$ and $Y \in \mathcal{Y}$, where $\mathbf{X}$ is the sequence of tokens that combine visual and text queries, and $Y$ represents the associated response tokens. The joint population is denoted by $P_{\mathbf{X}Y}$, with marginals $P_{\mathbf{X}}$, $P_Y$, and the conditional distribution $P_{Y|\mathbf{X}}$. For subsequent sections, $P_{\mathbf{X}Y}$ refers to the instruction tuning distribution which we consider as in-distribution (ID).

**MLLM and visual instruction tuning.** MLLM usually consists of three components: (1) a visual encoder, (2) a vision-to-language projector, and (3) an LLM that processes a multimodal input sequence to generate a valid textual output $y$ in response to an input query $\mathbf{x}$. An MLLM can be regarded as modeling a conditional distribution $P_\theta(y|\mathbf{x})$, where $\theta$ is the model parameters. To attain the multimodal conversation capability, MLLMs commonly undergo a phase so-called *visual instruction tuning* Liu et al. (2023); Dai et al. (2023) with an autoregressive objective as follows:

$$\min_{\theta \in \Theta} \mathbb{E}_{\mathbf{x}, y \sim P_{\mathbf{X}Y}} [\sum_{l=0}^{L} - \log P_\theta(y_l | \mathbf{x}, y_{<l})], \tag{1}$$

where $L$ is a sequence length and $y = (y_0, ..., y_L)$. After being trained by Eq. 1, MLLM produces a response given a query of any possible tasks represented by text.

**Evaluation of open-ended generations.** (M)LLM-as-a-judge method Zheng et al. (2023) is commonly adopted to evaluate open-ended generation. In this setup, a judge model produces preference scores or rankings for the responses given a query, model responses, and a scoring rubric. Among the evaluation metrics, the *win rate* (Eq. 2) is one of the most widely used and representative.

**Definition 2.1 (Win Rate)** *Given a parametric reward function $r : \mathcal{X} \times \mathcal{Y} \to \mathbb{R}$, the win rate (WR) of model $P_\theta$ w.r.t. $P_{\mathbf{X}Y}$ are defined as follows:*

$$\textit{WR}(P_{\mathbf{X}Y}; \theta) := \mathbb{E}_{\substack{\mathbf{x}, y \sim P_{\mathbf{X}Y} \\ \hat{y} \sim P_\theta(\cdot|\mathbf{x})}} [\mathbb{I}(r(\mathbf{x}, \hat{y}) > r(\mathbf{x}, y))], \tag{2}$$

*where $\mathbb{I}(\cdot)$ is the indicator function, and $r(\cdot, \cdot)$, can be any possible (multimodal) LLMs.*

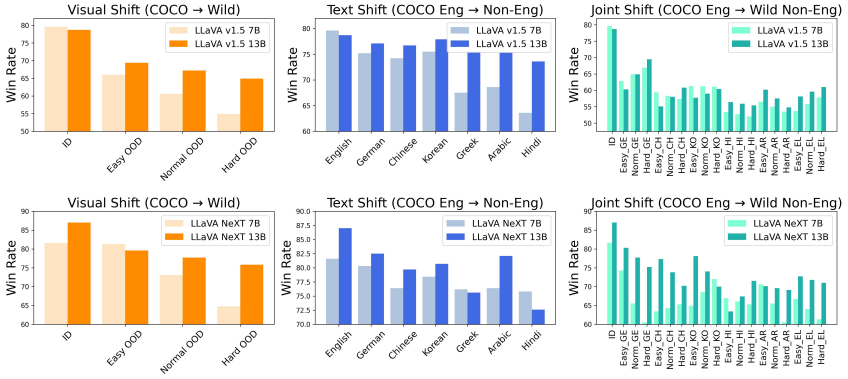


Figure 2: **Performance variation against varying distribution shifts.** We evaluated LLaVA v1.5 (top) and LLaVA NeXT (bottom) models on 27 out-of-distribution (OOD) variants of the LLaVA-Bench COCO (ID). Here, the $x$-axis is sorted by the severity of shifts between ID and OOD. There is a consistent trend, increased degrees of distribution shifts result in performance degradations.

## 3 MOTIVATION

**A systematic understanding of MLLM under distributional shifts.** While instruction-following MLLMs are designed to handle a diverse range of tasks, they often struggle with specialized domains Zhang et al. (2024a); Zhou et al. (2024), perform poorly on simple image classification tasks Zhai et al. (2024); Zhang et al. (2024b), and exhibit hallucinations Li et al. (2023b); Ye-Bin et al. (2025). We argue that the fundamental cause of these failure modes in MLLMs can be traced back to distribution shifts. Specifically, the poor performance on classification tasks and specialized distributions can be attributed to shifts between instruction tuning distribution $P_{\mathbf{X}Y}$ and evaluation distribution $Q_{\mathbf{X}Y}$. We comprehensively analyze three types of distributional shifts that can arise in MLLM:

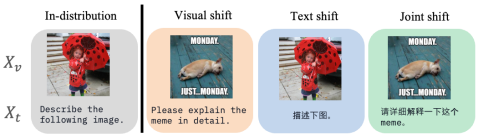


Figure 1: **Types of distribution shifts between train and evaluation of MLLMs.** We simulate visual, text, and joint shifts by controlling the shift of each input modality.

1. ***Visual shift***: the marginal distribution of visual query undergoes shift $D(P_{X_v} \| Q_{X_v}) \gg 0$, while that of text query remains largely unchanged $D(P_{X_t} \| Q_{X_t}) \approx 0$.
2. ***Text shift***: the marginal distribution of text query undergoes shift $D(P_{X_t} \| Q_{X_t}) \gg 0$, while that of visual query remains largely unchanged $D(P_{X_v} \| Q_{X_v}) \approx 0$.
3. ***Joint shift***: both visual and text queries suffer shifts simultaneously, and the relationship between visual and text queries may also shift $D(P_{\mathbf{X}} \| Q_{\mathbf{X}}) \gg 0$,

where $D$ denotes a divergence that measures the discrepancy between distributions $P$ and $Q$. For $M = (P + Q)/2$, one can measure the Kullback-Leibler (KL) divergence and Jensen-Shannon (JS) divergence as below:

$$D_{\mathrm{KL}}(P\|Q) = \mathbb{E}_{\mathbf{z}\sim P}[\log P(\mathbf{z})/Q(\mathbf{z})], \qquad D_{\mathrm{JS}}(P\|Q) = [D_{\mathrm{KL}}(P\|M) + D_{\mathrm{KL}}(Q\|M)]/2.$$

**Pilot study.** We hypothesize that: (1) performance degradation in MLLMs becomes more severe as $Q_{\mathbf{X}Y}$ deviates further from the $P_{\mathbf{X}Y}$; (2) the amount of total performance degradation can be factored into visual query shift and text query shift. To verify these, we design three types of shifts—visual shift, text shift, and joint shift—illustrated in Figure 1, and evaluate MLLMs under these shifts.

Specifically, we adopt LLaVA-1.5 Liu et al. (2023) and LLaVA-NeXT Liu et al. (2024a) in 7B and 13B sizes as our target MLLM, with LLaVA-Bench COCO Liu et al. (2023) serving as the ID dataset which is distributionally similar to the instruction tuning data. We adopt LLaVA-Bench Wild Liu et al. (2023) to vary the visual input, whereas applied language translation with GPT-4, e.g., from English to {Chinese, German, Chinese, Korean, Hindi, Arabic, and Greek}, to realize a shift in text query. We vary the severity of shifts by controlling the magnitude of perturbations in synthetic shift setup and partitioning a dataset based on mean embedding distance from ID samples in natural shift setup. Following Liu et al. (2023), we evaluate the performance using win rate (Eq. 2) with GPT-4 judge.

Figure 2 shows the performance variations of MLLMs under different types and magnitudes of distribution shifts, where the $x$-axis is sorted by the severity of shifts (more results from different types of shifts can be founded in Appendix D). Across all models, a consistent trend emerges: as the severity of the shift increases, the performance degradation becomes more significant. This trend robustly holds for both visual and text shifts. Joint shifts result in greater performance degradation, suggesting a complementary effect of shifts across modalities. *These consistent observations suggest that there might exist an underlying principle explaining the relationship between performance variation and distributional discrepancy, which motivates us to investigate the theoretical model behind these empirical results.*

**Our position.** Although there have been similar observations of performance degradation of MLLM under distribution shifts Achiam et al. (2023); Zhang et al. (2024a); Zhou et al. (2024); Zhang et al. (2024b), all of them present only the coarse empirical evaluation results without finer analysis on the underlying factor of those performance degradations. To the best of our knowledge, there is no formal framework to explain the performance variations of MLLMs in terms of distribution shifts—despite its crucial importance for ensuring reliable applications of MLLMs. To bridge this gap, we propose the ***first theoretical framework that characterizes MLLM performance variations under distribution shifts from an information-theoretic perspective***.

## 4 Information-theoretic Analysis on MLLM Performance Gap

In this section, we start with introducing the mutual information (MI) and its limitation as a metric in Sec. 4.1, and present a new metric on MLLM evaluation (Sec. 4.2). Then, we derive theorems based on it to characterize the MLLM performance gap under distribution shifts (Sec. 4.3).

### 4.1 Mutual Information for MLLM

A fundamental capability of MLLMs is their instruction-following property Ouyang et al. (2022)—a direct outcome of instruction-tuning, where the model is trained to generate responses that are aligned with the intent of a given input query or instruction. To evaluate instruction-following, we first consider the *mutual information* Shannon (1948) to measure the shared information between the query and the corresponding model response. Formally, for a joint distribution $P_{\mathbf{X}Y}$ over $\mathcal{X} \times \mathcal{Y}$, the mutual information with respect to $P_{\mathbf{X}Y}$ is defined as, $I(P_{\mathbf{X}Y}) := \mathbb{E}_{\mathbf{x},y\sim P_{\mathbf{X}Y}}[\log \frac{P_{\mathbf{X}Y}(\mathbf{x},y)}{P_{\mathbf{X}}(\mathbf{x})P_Y(y)}]$. MI is deeply related to the entropy, which is defined as $H(P_{\mathbf{X}}) := -\mathbb{E}_{\mathbf{x}\sim P_{\mathbf{X}}}[\log P_{\mathbf{X}}(\mathbf{x})]$. It is easy to check that $I(P_{\mathbf{X}Y}) = H(P_Y) - \mathbb{E}_{\mathbf{x}\sim P_{\mathbf{X}}}[H(P_{Y|\mathbf{X}=\mathbf{x}})]$. Intuitively, MI captures how much the response tells us about the query. One reason for considering MI is that the autoregressive objective in Eq. 1 effectively estimates MI (see Eq. 3).

**Visual instruction tuning effectively maximizes a lower bound of MI.** In Eq. 3, we show that the autoregressive objective for instruction tuning (Eq. 1) effectively estimates the lower bound of MI when the model's representation capacity is sufficiently high, i.e., when $\delta$ becomes small. Therefore, instruction tuning with autoregressive objective effectively maximizes a lower bound of MI between the input query and desired response as below, where $\delta = \mathbb{E}_{\mathbf{x}\sim P_{\mathbf{X}}}[D_{\mathrm{KL}}(P_{Y|\mathbf{X}=\mathbf{x}} \| P_\theta(\cdot|\mathbf{x}))]$.

$$I(P_{\mathbf{X}Y}) = \mathbb{E}_{\mathbf{x},y\sim P_{\mathbf{X}Y}}[\log P_\theta(y|\mathbf{x})] + H(P_Y) + \delta \geq \mathbb{E}_{\mathbf{x},y\sim P_{\mathbf{X}Y}}[\log P_\theta(y|\mathbf{x})]. \tag{3}$$

**Going from instruction tuning to test-time MI.** While $I(P_{\mathbf{X}Y})$ measures the MI between the input query and ground truth response from $P_{\mathbf{X}Y}$, one can measure MI between the input query and model response on the evaluation-time distribution. In particular, we use a tensor product $P_{\mathbf{X}} \otimes P_\theta$ to present this joint distribution between the input distribution $P_{\mathbf{X}}$ and *generated output* distribution $P_\theta(y|\mathbf{x})$: $P_{\mathbf{X}} \otimes P_\theta := P_{\mathbf{X}}(\mathbf{x})P_\theta(y|\mathbf{x})$, $\forall(\mathbf{x}, y) \in \mathcal{X} \times \mathcal{Y}$. Accordingly, the mutual information w.r.t. the joint distribution $P_{\mathbf{X}} \otimes P_\theta$ can be written as:

$$I(P_{\mathbf{X}} \otimes P_\theta) = H(\mathbb{E}_{\mathbf{x}\sim P_{\mathbf{X}}}[P_\theta(\cdot|\mathbf{x})]) - \mathbb{E}_{\mathbf{x}\sim P_{\mathbf{X}}}[H(P_\theta(\cdot|\mathbf{x}))]. \tag{4}$$

**Limitation of test-time MI under distribution shifts.** Although one could directly use $I(P_{\mathbf{X}} \otimes P_\theta)$, the mutual information between the input query and the model response, as a metric, the vanilla MI may not be suitable for scenarios involving distribution shifts. For example, consider the distribution $P_{\mathbf{X}}$ (e.g., general domain), and the distribution $Q_{\mathbf{X}}$ (e.g., medical domain). Suppose the MI w.r.t. model $P_\theta$ on $P_{\mathbf{X}}$, i.e., $I(P_{\mathbf{X}} \otimes P_\theta)$ is 2.0, while on the $Q_{\mathbf{X}}$, it is $I(Q_{\mathbf{X}} \otimes P_\theta) = 1.0$. Does this imply that model $P_\theta$ performs twice as poorly on $Q_{\mathbf{X}}$? The answer is unclear.

The challenge lies in the inherent variability of MI scales across data domains. Recall the formulation of $I(P_{\mathbf{X}} \otimes P_\theta)$ in Eq. 4, the first term $H(\mathbb{E}_{\mathbf{x}\sim P_{\mathbf{X}}}[P_\theta(\cdot|\mathbf{x})])$ represents the upper bound of MI and varies with the data domain; and the second term $\mathbb{E}_{\mathbf{x}\sim P_{\mathbf{X}}}[H(P_\theta(\cdot|\mathbf{x}))]$ reflects the input-output dependency and depends on the true data-generating process. For instance, given a fixed vocabulary, the responses from MLLM could contain more diverse words in a general domain whereas a narrower subset of words could be expected in the specialized domains such as medical. Then, $H(\mathbb{E}_{\mathbf{x}\sim P_{\mathbf{X}}}[P_\theta(\cdot|\mathbf{x})])$ and $\mathbb{E}_{\mathbf{x}\sim P_{\mathbf{X}}}[H(P_\theta(\cdot|\mathbf{x}))]$ would be larger in a general domain. Therefore, we argue that *a desired evaluation metric should disentangle the pure input-response relevance from the intrinsic characteristics of dataset*.

### 4.2 Effective Mutual Information for Reliable MLLM Evaluation

To remove the influence of the domain-dependent scale, we propose *effective mutual information* (EMI) as a remedy.

**Definition 4.1 (Effective Mutual Information (EMI))** *Given the joint distribution $P_{\mathbf{X}Y}$ and MLLM $P_\theta$ parameterized with $\theta$, the effective mutual information between the input and model response is defined as below,*

$$\textit{EMI}(P_{\mathbf{X}Y};\theta) := I(P_{\mathbf{X}} \otimes P_\theta) - I(P_{\mathbf{X}Y}). \tag{5}$$

Compared to the standard MI, $\text{EMI}(P_{\mathbf{X}Y};\theta)$ measures the "effective" relevance between the query $\mathbf{x}$ and the model response $\hat{y}$ by subtracting a ground truth MI $I(P_{\mathbf{X}Y})$ from $I(P_{\mathbf{X}} \otimes P_\theta)$. Refer to Figure 4 in Appendix B, for an intuitive example: by accounting for a baseline level of MI, EMI quantifies the extent to which the model captures the effective relevance between the input and output. The use of EMI as an evaluation metric for MLLMs can be further supported by (1) its analogy to the excess risk and effective robustness; and (2) its connection to win rate.

**Analogy to the excess risk and effective robustness.** The minimum achievable error varies depending on the data-generating process. To enable reliable model selection that is agnostic to data distributions, excess risk—defined as the difference between a model's risk and the minimum possible risk—has been extensively studied Castro & Nowak (2008); Koltchinskii (2010); Mohri (2018). More recently, Taori et al. (2020) introduced the concept of effective robustness to quantify the "effective" OOD generalization accuracy of classification models by subtracting their ID accuracy. The motivation behind EMI aligns with these concepts, i.e., mitigating the influence of external confounding effects that hinder the accurate measure of model performance. EMI ensures that the metric focuses on the model's effective ability to capture input-output relevance, independent of confounding effects from the data domain.

**Connection to win rate.** We also show that EMI is closely related to win rate (i.e., Eq. 2), a common metric used for evaluating MLLM generations. Conceptually, EMI quantifies the effective relevance between the input query and the model's response by accounting for the baseline information, while win rate measures the preference of the model's responses over a reference response. More formally, their connection can be mathematically established through the lens of a logit Bradley-Terry preference model (PM) formulation Bradley & Terry (1952); Hunter (2004), $\text{logit}P(\hat{y} \succ y|\mathbf{x})$, a smooth and differentiable proxy for the discrete win rate function. To be specific, we commonly use $\log P(\hat{y} \succ y|\mathbf{x})$ to train a reward model (RM) which is adopted to compute the win rate (Eq. 2). We compare both terms as below.

$$\begin{aligned}
\text{PM}(P_{\mathbf{X}Y};\theta) &:= \mathbb{E}_{\substack{\mathbf{x},y\sim P_{\mathbf{X}Y}\\ \hat{y}\sim P_\theta(\cdot|\mathbf{x})}}[\text{logit } P(\hat{y} \succ y|\mathbf{x})] = \mathbb{E}_{\substack{\mathbf{x},y\sim P_{\mathbf{X}Y}\\ \hat{y}\sim P_\theta(\cdot|\mathbf{x})}}[r(\mathbf{x},\hat{y}) - r(\mathbf{x},y)],\\
\text{RM}(P_{\mathbf{X}Y};\theta) &:= \mathbb{E}_{\substack{\mathbf{x},y\sim P_{\mathbf{X}Y}\\ \hat{y}\sim P_\theta(\cdot|\mathbf{x})}}[\log\ P(\hat{y} \succ y|\mathbf{x})] = \mathbb{E}_{\substack{\mathbf{x},y\sim P_{\mathbf{X}Y}\\ \hat{y}\sim P_\theta(\cdot|\mathbf{x})}}[\log \sigma(r(\mathbf{x},\hat{y}) - r(\mathbf{x},y))],
\end{aligned} \tag{6}$$

where $r(\cdot,\cdot)$ is the latent score function so-called reward model that generates preference for $(\mathbf{x}, y)$. It is clear that

$$\begin{aligned}
\text{PM}(P_{\mathbf{X}Y};\theta) &= \text{RM}(P_{\mathbf{X}Y};\theta) - \log(1 - e^{\text{RM}(P_{\mathbf{X}Y};\theta)}),\\
\text{RM}(P_{\mathbf{X}Y};\theta) &= \text{PM}(P_{\mathbf{X}Y};\theta) - \log(1 + e^{\text{PM}(P_{\mathbf{X}Y};\theta)}).
\end{aligned}$$

Therefore, $\text{PM}(P_{\mathbf{X}Y};\theta)$ and $\text{RM}(P_{\mathbf{X}Y};\theta)$ exhibit a mutual equivalence, i.e., *increase in PM$(P_{\mathbf{X}Y};\theta)$ corresponds to the increase in RM$(P_{\mathbf{X}Y};\theta)$, and vice versa.* In Theorem 4.2, we establish an upper bound for the absolute difference between EMI and $\text{PM}(P_{\mathbf{X}Y};\theta)$, thereby demonstrating their closeness while ultimately highlighting the connection between EMI and win rate.

**Theorem 4.2** *Given a distribution $P_{\mathbf{X}Y}$ and an MLLM $P_\theta$, if $\mathbb{E}_{\mathbf{x}\sim P_{\mathbf{X}}}[D_{\mathrm{KL}}(P_\theta(\cdot|\mathbf{x})\|P_{Y|\mathbf{X}=\mathbf{x}})] \leq \delta$, and let the reward function $r(\mathbf{x}, y)$ be $\log P_{Y|\mathbf{X}=\mathbf{x}}(y)$, then*

$$|\mathit{EMI}(P_{\mathbf{X}Y};\theta) - \mathit{PM}(P_{\mathbf{X}Y};\theta)| \leq \delta + 4.4\delta^{\frac{1}{8}}.$$

Intuitively, Theorem 4.2 shows that if MLLM $P_\theta$ can approximate the given distribution $P_{\mathbf{X}Y}$ with approximate error $\delta$, the difference between EMI and PM can be bounded by a small term w.r.t. the approximate error $\delta$. Furthermore, assuming that the model class $\{P_\theta : \forall\theta \in \Theta\}$ has sufficient expressive power (i.e., Eq. 11), we can derive an additional bound for the case of the optimal solution of autoregressive objective (i.e., Eq. 1), as shown in Theorem E.2

### 4.3 Characterizing MLLM Performance Gap via EMI Difference

Now, based on EMI, we are ready to establish formal guarantees on the performance gap of MLLM via *effective mutual information difference* (EMID). EMID is defined as the difference between the EMI on the ID distribution $P_{\mathbf{X}Y}$ and the OOD distribution $Q_{\mathbf{X}Y}$, as follows:

$$\mathrm{EMID}(P_{\mathbf{X}Y}, Q_{\mathbf{X}Y};\theta) := \mathrm{EMI}(P_{\mathbf{X}Y};\theta) - \mathrm{EMI}(Q_{\mathbf{X}Y};\theta). \tag{7}$$

To elucidate the key insight and provide a clear foundation, we begin by analyzing a simple scenario where the conditional variables remain consistent across both ID and OOD distributions. In this case, we can derive an upper bound for EMID, as stated in Theorem 4.3. This bound enables us to quantify the maximum performance gap of MLLM over two distributions by measuring the severity of the marginal distribution shift over visual and language modalities.

**Theorem 4.3 (Simplified Scenario)** *Given an MLLM $P_\theta$ and distributions $P_{\mathbf{X}Y}$, $Q_{\mathbf{X}Y}$ which have consistent conditional distributions over variables $X_v|X_t$, $X_t|X_v$, and $Y|\mathbf{X}$, if there exist some constants $\delta_P$ and $\delta_Q$ such that $D_{\mathrm{JS}}(P_{Y_\theta}\|P_Y) \leq \delta_P$, and $D_{\mathrm{JS}}(Q_{Y_\theta}\|Q_Y) \leq \delta_Q$, and denote $P_{Y_\theta} = \mathbb{E}_{P_{\mathbf{X}}}[P_\theta(\cdot|\mathbf{x})]$ and $Q_{Y_\theta} = \mathbb{E}_{Q_{\mathbf{X}}}[P_\theta(\cdot|\mathbf{x})]$, then EMID$(P_{\mathbf{X}Y}, Q_{\mathbf{X}Y};\theta)$ is upper bounded by*

$$\widehat{H}\left(D_{\mathrm{JS}}^{\frac{1}{2}}(P_{X_v}\|Q_{X_v}) + D_{\mathrm{JS}}^{\frac{1}{2}}(P_{X_t}\|Q_{X_t})\right) + 8\Delta^{\frac{1}{4}}, \tag{8}$$

*where $\widehat{H} = \max_{\mathbf{x}\in\mathcal{X}}[H(Q_{Y|\mathbf{X}=\mathbf{x}}) + H(P_\theta(\cdot|\mathbf{x}))]$ and $\Delta = \delta_P + \delta_Q$.*

> **Implication.** Theorem 4.3 implies that in the simplified scenario, EMID depends on two main factors: (1) the divergence between the marginal distributions of the visual and textual inputs; (2) the divergence between the model's predictions and the true output distributions, encapsulated by $\delta_P$ and $\delta_Q$.

Theorem 4.3 naturally captures special cases such as visual-only or text-only input shifts. For a visual-only input shift, where $D_{\mathrm{JS}}(P_{X_t}\|Q_{X_t}) = 0$, the EMID upper bound primarily depends on the divergence between the visual input distributions. Similarly, for a text-only input shift, the bound reflects the divergence in the textual input distributions. The two cases not only underscore the flexibility of Theorem 4.3 in isolating and quantifying the impact of modality-specific distribution shifts on model performance but also highlight the importance of visual and text input shifts on it. In Appendix E, we further provide a looser yet better interpretable version of this upper bound (Corollary E.12) by replacing the $\Delta$ into the discrepancy terms between model output and ground truth conditional distributions.

**General scenario.** Moving beyond the simplified scenario, we now consider the general scenario where no assumptions are made about the consistency of conditional distributions across ID and OOD settings. This more realistic scenario accommodates shifts not only in the marginal distributions of visual and textual inputs but also in their conditional dependencies and the relationships between inputs and outputs. By relaxing these constraints, we aim to capture the full complexity of distributional shifts encountered in practice and analyze how such shifts collectively influence the performance gap of MLLMs. The formal upper bound is provided in Theorem 4.4.

**Theorem 4.4 (General Scenario)** *Given $P_{\mathbf{X}Y}$ and $Q_{\mathbf{X}Y}$ distributions and an MLLM $P_\theta$, if there exist some constants $\delta_P$ and $\delta_Q$ such that $D_{\mathrm{JS}}(P_{Y_\theta}\|P_Y) \leq \delta_P$, and $D_{\mathrm{JS}}(Q_{Y_\theta}\|Q_Y) \leq \delta_Q$, and*

*denote* $P_{Y_\theta} = \mathbb{E}_{P_{\mathbf{X}}}[P_\theta(\cdot|\mathbf{x})]$ *and* $Q_{Y_\theta} = \mathbb{E}_{Q_{\mathbf{X}}}[P_\theta(\cdot|\mathbf{x})]$, *then EMID*$(P_{\mathbf{X}Y}, Q_{\mathbf{X}Y}; \theta)$ *is upper bounded by*

$$\widehat{H}\left(D_{\mathrm{JS}}^{\frac{1}{2}}(P_{X_v}||Q_{X_v}) + D_{\mathrm{JS}}^{\frac{1}{2}}(P_{X_t}||Q_{X_t})\right) + \widehat{H}\left(\bar{D}_{\mathrm{JS}}^{\frac{1}{2}}(P_{X_t|X_v}\|Q_{X_t|X_v}) + \bar{D}_{\mathrm{JS}}^{\frac{1}{2}}(P_{X_v|X_t}\|Q_{X_v|X_t})\right)$$
$$+4\mathbb{E}_{\mathbf{x}\sim P_{\mathbf{X}}} D_{\mathrm{JS}}^{\frac{1}{4}}(P_{Y|\mathbf{X}=\mathbf{x}}\|Q_{Y|\mathbf{X}=\mathbf{x}}) + 8\Delta^{\frac{1}{4}},$$

*where* $\widehat{H} = \max_{\mathbf{x}\in\mathcal{X}}[H(Q_{Y|\mathbf{X}=\mathbf{x}}) + H(P_\theta(\cdot|\mathbf{x}))]$, $\Delta = \delta_P + \delta_Q$, *and* $\bar{D}_{\mathrm{JS}}(P_{X|X'}||Q_{X|X'}) := \mathbb{E}_{\mathbf{x}\sim P_{X'}}[D_{\mathrm{JS}}(P_{X|X'=\mathbf{x}}\|Q_{X|X'=\mathbf{x}})] + \mathbb{E}_{\mathbf{x}\sim Q_{X'}}[D_{\mathrm{JS}}(P_{X|X'=\mathbf{x}}\|Q_{X|X'=\mathbf{x}})]$.

**Implication.** Compared to Theorem 4.3, Theorem 4.4 indicates that, in the general case, EMID is also influenced by divergences in conditional distributions. Specifically, EMID is upper bounded by marginal distribution shifts in visual and textual inputs ($X_v$ and $X_t$); divergence between marginal output and model response distributions; shifts in conditional dependencies ($X_v|X_t$ and $X_t|X_v$); and a shift between conditional distributions for $Y|\mathbf{X}$.

Although Theorem 4.4 holds for broader cases, Theorem 4.3 is much simpler to analyze. Thus, we focus on the validation of Theorem 4.3 in the following section. If we have some knowledge of the data-generating process of $P_{\mathbf{X}Y}$ and $Q_{\mathbf{X}Y}$, we can choose the one that is suitable for a given setup. In summary, both Theorem 4.3 and 4.4 *provide an analytic tool to characterize the performance gap of MLLM, representing the first formal framework for evaluating MLLM under distribution shifts.*

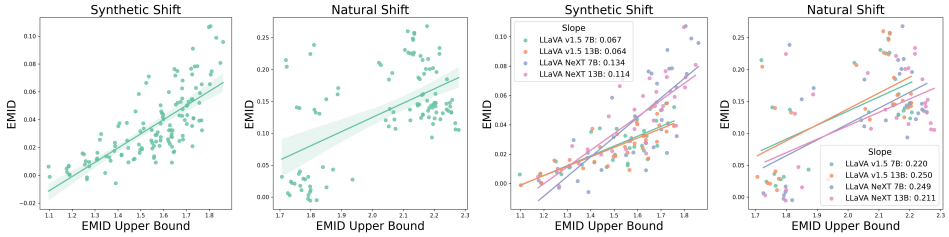


Figure 3: **Scatter plot with regression line between empirical estimates of EMID and its upper bound.** Over the 34 synthetic and 27 natural distribution shift scenarios, we evaluate four MLLMs and get 136 cases and 108 cases of synthetic shifts and natural shifts, respectively, for visualizing EMID and upper bound estimates. The two panels on the left show results for all four models, whereas the right ones distinguish them per model with fitter linear regression coefficients (Slope).

## 5 Empirical Validation on Real Benchmark

**Setup.** As done in the pilot experiments (Figure 2 and 5), we used LLaVA v1.5 Liu et al. (2024a) and LLaVA NeXT Liu et al. (2024b) in 7B and 13B sizes and evaluated them on the LLaVA-Bench COCO and LLaVA-Bench Wild Liu et al. (2023) datasets for assessing open-ended generation. To comprehensively examine diverse types of shifts, we further simulate synthetic distribution shifts as well as natural distribution shifts. For synthetic shifts, we consider 7 visual scenarios (1 ID case + 2 synthetic perturbation types at 3 severity levels), and 5 text scenarios (1 ID case + 2 synthetic perturbation types at 2 severity levels), resulting in $7 \times 5 = 35$ synthetic scenarios, where 1 scenario is ID and the other 34 are OOD cases. For natural shifts, we use 4 visual scenarios (1 ID + 3 OOD difficulty levels) and 7 text scenarios (1 ID-English + 6 languages), yielding $4 \times 7 = 28$ natural scenarios. **This comprehensive design covers a total of 34 synthetic and 27 natural shifts**. See Table 1 for the description.

Table 1: **Summary of shift scenarios.**

| Type | Strategy (# of category) |
|---|---|
| Synthetic visual shift (COCO Images) | Perturbation (2): Defocus blur, frost<br>Severity (3): Weak, Normal, Strong |
| Synthetic text shift | Perturbation (2): Typo, Word Replacement<br>Severity (2): Weak, Strong |
| Natural visual shift (in-the-wild Images) | LLaVA-Bench in-the-wild<br>Split (3): Easy, Normal, Hard |
| Natural text shift | Translation (6): GE, CH, KO, EL, AR, HI |

**Estimation of MI and JSD.** For the empirical realization of our theoretical statements, we adopt a popular neural estimator for MI, CLUB Cheng et al. (2020) to compute empirical EMID, and a JS divergence estimator, RJSD Hoyos-Osorio & Sanchez-Giraldo (2023), to compute empirical EMID and its upper-bound (see Appendix C for details). Experiments with 23 alternative implementations derived consistent conclusions (Please refer to Table 4 and 5).

**Correlation between win rate and EMI.** We first conduct the Spearman correlation analysis and Kendall's tau analysis between the win rate and our empirical estimates of EMI. In Table 2, we can see that EMI estimates exhibit a strong correlation with win rate, both in terms of absolute coefficient and $p$-value, across all models. This empirical evidence validates the theoretical connection between EMI and win rate discussed in Theorem 4.2. Therefore, our EMI can be used as a reliable and cost-efficient alternative to win rate for MLLM evaluation with theoretical guarantees.

Table 2: **Spearman rank correlation and Kendall's tau between win rate and EMI.** We conduct correlation analysis between the win rate (Eq. 2) and EMI (Eq. 5).

| | Model | Spearman $\rho$ | Spearman $p$-val | Kendall $\tau$ | Kendall $p$-val |
|---|---|---|---|---|---|
| Synthetic | LLaVA v1.5 7B | 0.794 | <0.001 | 0.604 | <0.001 |
| | LLaVA v1.5 13B | 0.652 | <0.001 | 0.483 | <0.001 |
| | LLaVA NeXT 7B | 0.738 | <0.001 | 0.564 | <0.001 |
| | LLaVA NeXT 13B | 0.726 | <0.001 | 0.527 | <0.001 |
| Natural | LLaVA v1.5 7B | 0.610 | 0.001 | 0.450 | 0.001 |
| | LLaVA v1.5 13B | 0.720 | <0.001 | 0.575 | <0.001 |
| | LLaVA NeXT 7B | 0.593 | 0.001 | 0.435 | 0.001 |
| | LLaVA NeXT 13B | 0.457 | 0.014 | 0.321 | 0.017 |

Table 3: **Pearson correlation analysis between EMID and its upper bound.** We provide Pearson $r$ and $p$-value between the empirical estimates of EMID (Eq. 7) and its upper bound (Eq. 8).

| Model | Synthetic Pearson $r$ | Synthetic $p$-val | Natural Pearson $r$ | Natural $p$-val |
|---|---|---|---|---|
| LLaVA v1.5 7B | 0.755 | <0.001 | 0.553 | 0.003 |
| LLaVA v1.5 13B | 0.785 | <0.001 | 0.638 | <0.001 |
| LLaVA v1.5 7B | 0.742 | <0.001 | 0.594 | 0.001 |
| LLaVA v1.5 13B | 0.807 | <0.001 | 0.550 | 0.003 |
| All models | 0.746 | <0.001 | 0.565 | <0.001 |

**Verification of bound.** We now validate our main Theorem. Figure 3 (left two) shows the scatter plots comparing EMID with its upper bound across four models, each evaluated over 34 and 27 synthetic and natural distribution shifts. We see a clear trend between EMID and its upper bound in the synthetic shift where we could directly control the severity of shifts. While the natural shift setup is noisier, a similar overall trend is observed. Meanwhile, our bounds depend on the distributional discrepancy between the model's response $\hat{y}$ and the ground truth response $y$. Thus, they naturally induce different bounds for each MLLM. The right panel of Figure 3 presents model-wise plots with linear regression coefficients, where we observe that each model has a different degree of performance sensitivity against shifts. Pearson correlation analysis results in Table 3 further confirm statistically significant correlations between EMID and its upper bound, supporting the validity of the theorem.

## 6 Discussion

We urged the development of a formal framework to understand MLLMs under distribution shifts which is unexplored yet crucial for reliable AI in the wild. As a first step for this, we devised EMI as a metric for MLLM evaluation and showed its theoretical connection to an existing standard metric, win rate. Then, we provide a theoretical upper bound for an MLLM's EMI difference between ID and OOD that consists of JS divergence terms for marginal and conditional distributions of input/output variables. Through experiments on a benchmark spanning 61 distribution shifts, we show the correlation between win rate and EMI, and further show the correlation between EMI difference and its upper bound thereby empirically verifying our theoretical upper bound.

**Practical implication.** As shown in Table 2, EMI strongly correlates with win rate. Compared to the win rate, the MI estimator can be computed more efficiently without relying on computationally expensive judge LLM Achiam et al. (2023) (see Appendix D.5 for details). Therefore, EMI can be leveraged as a cost-efficient and theoretically grounded evaluation metric that measures effective relevance between multimodal queries and open-ended responses. Besides, the upper bound of EMID can be adopted as a regularizer during post-training or test-time adaptation of MLLM to improve its robustness to distribution shifts Li et al. (2023a).

**Limitation and future work.** Although input-output relevance measured by EMI is one of the most important properties for instruction-following assistant models, other crucial quality attributes are not captured by the form of relevance term. Extending the theory to support evaluation across multiple facets of MLLM will be promising future work direction. Besides, we have simulated some intuitive types of distribution shifts with the simplified assumption for data structure, while leaving some complex shifts driven by spurious correlation Simon (1954) that may be covered by Theorem 4.4. Validation of theorems on such non-trivial distribution shifts could be an important extension.

### ACKNOWLEDGMENTS

We thank ICLR QUESTION workshop anonymous reviewers for their reading and feedback. This work is supported by the AFOSR Young Investigator Program under award number FA9550-23-1-0184, National Science Foundation (NSF) Award No. IIS-2237037 and IIS-2331669, Office of Naval Research under grant number N00014-23-1-2643, and Schmidt Science Foundation.

## REFERENCES

Josh Achiam, Steven Adler, Sandhini Agarwal, Lama Ahmad, Ilge Akkaya, Florencia Leoni Aleman, Diogo Almeida, Janko Altenschmidt, Sam Altman, Shyamal Anadkat, et al. Gpt-4 technical report. *arXiv preprint arXiv:2303.08774*, 2023.

Alexander A Alemi, Ian Fischer, Joshua V Dillon, and Kevin Murphy. Deep variational information bottleneck. *arXiv preprint arXiv:1612.00410*, 2016.

Mohamed Ishmael Belghazi, Aristide Baratin, Sai Rajeshwar, Sherjil Ozair, Yoshua Bengio, Aaron Courville, and Devon Hjelm. Mutual information neural estimation. In *Proceedings of the 35th International Conference on Machine Learning*, pp. 531–540. PMLR, 2018.

Ralph Allan Bradley and Milton E Terry. Rank analysis of incomplete block designs: I. the method of paired comparisons. *Biometrika*, 39(3/4):324–345, 1952.

Yuheng Bu, Shaofeng Zou, Yingbin Liang, and Venugopal V Veeravalli. Estimation of kl divergence: Optimal minimax rate. *IEEE Transactions on Information Theory*, 64(4):2648–2674, 2018.

Rui M Castro and Robert D Nowak. Minimax bounds for active learning. *IEEE Transactions on Information Theory*, 54(5):2339–2353, 2008.

Hanjie Chen, Faeze Brahman, Xiang Ren, Yangfeng Ji, Yejin Choi, and Swabha Swayamdipta. Rev: Information-theoretic evaluation of free-text rationales. In *Proceedings of the 61st Annual Meeting of the Association for Computational Linguistics (Volume 1: Long Papers)*, pp. 2007–2030, 2023.

Xi Chen, Yan Duan, Rein Houthooft, John Schulman, Ilya Sutskever, and Pieter Abbeel. Infogan: Interpretable representation learning by information maximizing generative adversarial nets. *Advances in neural information processing systems*, 29, 2016.

Pengyu Cheng, Weituo Hao, Shuyang Dai, Jiachang Liu, Zhe Gan, and Lawrence Carin. Club: A contrastive log-ratio upper bound of mutual information. In *International conference on machine learning*, pp. 1779–1788. PMLR, 2020.

Pengyu Cheng, Weituo Hao, Siyang Yuan, Shijing Si, and Lawrence Carin. Fairfil: Contrastive neural debiasing method for pretrained text encoders. In *International Conference on Learning Representations*, 2021.

A Conneau. Unsupervised cross-lingual representation learning at scale. *arXiv preprint arXiv:1911.02116*, 2019.

Wenliang Dai, Junnan Li, Dongxu Li, Anthony Meng Huat Tiong, Junqi Zhao, Weisheng Wang, Boyang Li, Pascale Fung, and Steven Hoi. Instructblip: towards general-purpose vision-language models with instruction tuning. In *Proceedings of the 37th International Conference on Neural Information Processing Systems*, pp. 49250–49267, 2023.

Marco Federici, Ryota Tomioka, and Patrick Forré. An information-theoretic approach to distribution shifts. *Advances in Neural Information Processing Systems*, 34:17628–17641, 2021.

Andrew M Fraser and Harry L Swinney. Independent coordinates for strange attractors from mutual information. *Physical review A*, 33(2):1134, 1986.

Sachin Goyal, Ananya Kumar, Sankalp Garg, Zico Kolter, and Aditi Raghunathan. Finetune like you pretrain: Improved finetuning of zero-shot vision models. In *Proceedings of the IEEE/CVF Conference on Computer Vision and Pattern Recognition*, pp. 19338–19347, 2023.

Zhongyi Han, Guanglin Zhou, Rundong He, Jindong Wang, Tailin Wu, Yilong Yin, Salman Khan, Lina Yao, Tongliang Liu, and Kun Zhang. How well does gpt-4v (ision) adapt to distribution shifts? a preliminary investigation. In *ICLR 2024 Workshop on Mathematical and Empirical Understanding of Foundation Models*, 2024.

Jack Hessel, Ari Holtzman, Maxwell Forbes, Ronan Le Bras, and Yejin Choi. Clipscore: A reference-free evaluation metric for image captioning. In *Proceedings of the 2021 Conference on Empirical Methods in Natural Language Processing*. Association for Computational Linguistics, 2021.

John Hewitt, Kawin Ethayarajh, Percy Liang, and Christopher D Manning. Conditional probing: measuring usable information beyond a baseline. In *Proceedings of the 2021 Conference on Empirical Methods in Natural Language Processing*, pp. 1626–1639, 2021.

Jhoan Keider Hoyos and Luis Gonzalo Sanchez Giraldo. A kernel two-sample test with the representation jensen-shannon divergence. In *Latinx in AI @ NeurIPS 2024*, 2024. URL `https://openreview.net/forum?id=bKZbWy3DnR`.

Jhoan K Hoyos-Osorio and Luis G Sanchez-Giraldo. The representation jensen-shannon divergence. *arXiv preprint arXiv:2305.16446*, 2023.

David R Hunter. Mm algorithms for generalized bradley-terry models. *The annals of statistics*, 32(1): 384–406, 2004.

Ting Jiang, Minghui Song, Zihan Zhang, Haizhen Huang, Weiwei Deng, Feng Sun, Qi Zhang, Deqing Wang, and Fuzhen Zhuang. E5-v: Universal embeddings with multimodal large language models. *arXiv preprint arXiv:2407.12580*, 2024.

Haotian Ju, Dongyue Li, and Hongyang R Zhang. Robust fine-tuning of deep neural networks with hessian-based generalization guarantees. In Kamalika Chaudhuri, Stefanie Jegelka, Le Song, Csaba Szepesvari, Gang Niu, and Sivan Sabato (eds.), *Proceedings of the 39th International Conference on Machine Learning*, volume 162 of *Proceedings of Machine Learning Research*, pp. 10431–10461. PMLR, 17–23 Jul 2022.

Seungone Kim, Jamin Shin, Yejin Cho, Joel Jang, Shayne Longpre, Hwaran Lee, Sangdoo Yun, Seongjin Shin, Sungdong Kim, James Thorne, et al. Prometheus: Inducing fine-grained evaluation capability in language models. In *The Twelfth International Conference on Learning Representations*, 2024.

Vladimir Koltchinskii. Rademacher complexities and bounding the excess risk in active learning. *The Journal of Machine Learning Research*, 11:2457–2485, 2010.

Lingpeng Kong, Cyprien de Masson d'Autume, Lei Yu, Wang Ling, Zihang Dai, and Dani Yogatama. A mutual information maximization perspective of language representation learning. In *International Conference on Learning Representations*, 2020.

Alexander Kraskov, Harald Stögbauer, and Peter Grassberger. Estimating mutual information. *Physical Review E—Statistical, Nonlinear, and Soft Matter Physics*, 69(6):066138, 2004.

Ananya Kumar, Aditi Raghunathan, Robbie Jones, Tengyu Ma, and Percy Liang. Fine-tuning can distort pretrained features and underperform out-of-distribution. In *International Conference on Learning Representations*, 2022.

Chunyuan Li, Cliff Wong, Sheng Zhang, Naoto Usuyama, Haotian Liu, Jianwei Yang, Tristan Naumann, Hoifung Poon, and Jianfeng Gao. Llava-med: Training a large language-and-vision assistant for biomedicine in one day. *Advances in Neural Information Processing Systems*, 36, 2024.

Moxin Li, Wenjie Wang, Fuli Feng, Yixin Cao, Jizhi Zhang, and Tat-Seng Chua. Robust prompt optimization for large language models against distribution shifts. In *Proceedings of the 2023 Conference on Empirical Methods in Natural Language Processing*, pp. 1539–1554, 2023a.

Yifan Li, Yifan Du, Kun Zhou, Jinpeng Wang, Xin Zhao, and Ji-Rong Wen. Evaluating object hallucination in large vision-language models. In *Proceedings of the 2023 Conference on Empirical Methods in Natural Language Processing*, pp. 292–305, 2023b. URL https://aclanthology.org/2023.emnlp-main.20.

Yingzhen Li and Richard E Turner. Rényi divergence variational inference. *Advances in neural information processing systems*, 29, 2016.

Yiming Liang, Tianyu Zheng, Xinrun Du, Ge Zhang, Xingwei Qu, Xiang Yue, Chujie Zheng, Jiaheng Liu, Lei Ma, Wenhu Chen, et al. Aligning instruction tuning with pre-training. *arXiv preprint arXiv:2501.09368*, 2025.

Feng Liu, Wenkai Xu, Jie Lu, Guangquan Zhang, Arthur Gretton, and Danica J Sutherland. Learning deep kernels for non-parametric two-sample tests. In *International conference on machine learning*, pp. 6316–6326. PMLR, 2020.

Haotian Liu, Chunyuan Li, Qingyang Wu, and Yong Jae Lee. Visual instruction tuning. *Conference on Neural Information Processing Systems (NeurIPS)*, 36, 2023.

Haotian Liu, Chunyuan Li, Yuheng Li, and Yong Jae Lee. Improved baselines with visual instruction tuning. In *Proceedings of the IEEE/CVF Conference on Computer Vision and Pattern Recognition*, pp. 26296–26306, 2024a.

Haotian Liu, Chunyuan Li, Yuheng Li, Bo Li, Yuanhan Zhang, Sheng Shen, and Yong Jae Lee. Llava-next: Improved reasoning, ocr, and world knowledge, January 2024b.

Mehryar Mohri. Foundations of machine learning, 2018.

XuanLong Nguyen, Martin J Wainwright, and Michael I Jordan. Estimating divergence functionals and the likelihood ratio by convex risk minimization. *IEEE Transactions on Information Theory*, 56(11):5847–5861, 2010.

Changdae Oh, Mijoo Kim, Hyesu Lim, Junhyeok Park, Euiseog Jeong, Zhi-Qi Cheng, and Kyungwoo Song. Towards calibrated robust fine-tuning of vision-language models. *Advances in Neural Information Processing Systems*, 37, 2025a.

Changdae Oh, Yixuan Li, Kyungwoo Song, Sangdoo Yun, and Dongyoon Han. Dawin: Training-free dynamic weight interpolation for robust adaptation. In *The Thirteenth International Conference on Learning Representations*, 2025b.

Aaron van den Oord, Yazhe Li, and Oriol Vinyals. Representation learning with contrastive predictive coding. *arXiv preprint arXiv:1807.03748*, 2018.

Long Ouyang, Jeffrey Wu, Xu Jiang, Diogo Almeida, Carroll Wainwright, Pamela Mishkin, Chong Zhang, Sandhini Agarwal, Katarina Slama, Alex Ray, et al. Training language models to follow instructions with human feedback. *Advances in neural information processing systems*, 35:27730–27744, 2022.

Liam Paninski. Estimation of entropy and mutual information. *Neural computation*, 15(6):1191–1253, 2003.

Mark S Pinsker. Information and information stability of random variables and processes. *Holden-Day*, 1964.

Ben Poole, Sherjil Ozair, Aaron Van Den Oord, Alex Alemi, and George Tucker. On variational bounds of mutual information. In *International Conference on Machine Learning*, pp. 5171–5180. PMLR, 2019.

Alec Radford, Jong Wook Kim, Chris Hallacy, Aditya Ramesh, Gabriel Goh, Sandhini Agarwal, Girish Sastry, Amanda Askell, Pamela Mishkin, Jack Clark, et al. Learning transferable visual models from natural language supervision. In *International conference on machine learning*, pp. 8748–8763. PMLR, 2021.

Claude Elwood Shannon. A mathematical theory of communication. *The Bell system technical journal*, 27(3):379–423, 1948.

Changjian Shui, Qi Chen, Jun Wen, Fan Zhou, Christian Gagné, and Boyu Wang. A novel domain adaptation theory with jensen–shannon divergence. *Knowledge-Based Systems*, 257:109808, 2022.

Ravid Shwartz-Ziv and Naftali Tishby. Opening the black box of deep neural networks via information. *arXiv preprint arXiv:1703.00810*, 2017.

Herbert A. Simon. Spurious correlation: A causal interpretation. *Journal of the American Statistical Association*, 49(267):467–479, 1954.

Mathieu Sinn and Ambrish Rawat. Non-parametric estimation of jensen-shannon divergence in generative adversarial network training. In *International Conference on Artificial Intelligence and Statistics*, pp. 642–651. PMLR, 2018.

Taylor Sorensen, Joshua Robinson, Christopher Rytting, Alexander Shaw, Kyle Rogers, Alexia Delorey, Mahmoud Khalil, Nancy Fulda, and David Wingate. An information-theoretic approach to prompt engineering without ground truth labels. In *Proceedings of the 60th Annual Meeting of the Association for Computational Linguistics (Volume 1: Long Papers)*, pp. 819–862, 2022.

Sreejith Sreekumar and Ziv Goldfeld. Neural estimation of statistical divergences. *Journal of machine learning research*, 23(126):1–75, 2022.

Bharath K. Sriperumbudur, Kenji Fukumizu, Arthur Gretton, Bernhard Schölkopf, and Gert R. G. Lanckriet. On the empirical estimation of integral probability metrics. *Electronic Journal of Statistics*, 6:1550 – 1599, 2012.

Rohan Taori, Achal Dave, Vaishaal Shankar, Nicholas Carlini, Benjamin Recht, and Ludwig Schmidt. Measuring robustness to natural distribution shifts in image classification. *Advances in Neural Information Processing Systems*, 33:18583–18599, 2020.

Kiran K Thekumparampil, Ashish Khetan, Zinan Lin, and Sewoong Oh. Robustness of conditional gans to noisy labels. In S. Bengio, H. Wallach, H. Larochelle, K. Grauman, N. Cesa-Bianchi, and R. Garnett (eds.), *Advances in Neural Information Processing Systems*, volume 31. Curran Associates, Inc., 2018. URL https://proceedings.neurips.cc/paper_files/paper/2018/file/565e8a413d0562de9ee4378402d2b481-Paper.pdf.

Junjiao Tian, Zecheng He, Xiaoliang Dai, Chih-Yao Ma, Yen-Cheng Liu, and Zsolt Kira. Trainable projected gradient method for robust fine-tuning. In *Proceedings of the IEEE/CVF Conference on Computer Vision and Pattern Recognition*, pp. 7836–7845, 2023.

Michael Tschannen, Josip Djolonga, Paul K. Rubenstein, Sylvain Gelly, and Mario Lucic. On mutual information maximization for representation learning. In *International Conference on Learning Representations*, 2020.

Aayush Atul Verma, Amir Saeidi, Shamanthak Hegde, Ajay Therala, Fenil Denish Bardoliya, Nagaraju Machavarapu, Shri Ajay Kumar Ravindhiran, Srija Malyala, Agneet Chatterjee, Yezhou Yang, et al. Evaluating multimodal large language models across distribution shifts and augmentations. In *Proceedings of the IEEE/CVF Conference on Computer Vision and Pattern Recognition*, pp. 5314–5324, 2024.

Martin J Wainwright. *High-dimensional statistics: A non-asymptotic viewpoint*, volume 48. Cambridge university press, 2019.

Boxin Wang, Shuohang Wang, Yu Cheng, Zhe Gan, Ruoxi Jia, Bo Li, and Jingjing Liu. Info{bert}: Improving robustness of language models from an information theoretic perspective. In *International Conference on Learning Representations*, 2021.

Mitchell Wortsman, Gabriel Ilharco, Jong Wook Kim, Mike Li, Simon Kornblith, Rebecca Roelofs, Raphael Gontijo Lopes, Hannaneh Hajishirzi, Ali Farhadi, Hongseok Namkoong, et al. Robust fine-tuning of zero-shot models. In *Proceedings of the IEEE/CVF conference on computer vision and pattern recognition*, pp. 7959–7971, 2022.

Yuhong Yang and Andrew Barron. Information-theoretic determination of minimax rates of convergence. *Annals of Statistics*, pp. 1564–1599, 1999.

Moon Ye-Bin, Nam Hyeon-Woo, Wonseok Choi, and Tae-Hyun Oh. Beaf: Observing before-after changes to evaluate hallucination in vision-language models. In *European Conference on Computer Vision*, pp. 232–248. Springer, 2025.

Weizhe Yuan, Graham Neubig, and Pengfei Liu. Bartscore: Evaluating generated text as text generation. *Advances in Neural Information Processing Systems*, 34:27263–27277, 2021.

Yuexiang Zhai, Shengbang Tong, Xiao Li, Mu Cai, Qing Qu, Yong Jae Lee, and Yi Ma. Investigating the catastrophic forgetting in multimodal large language model fine-tuning. In *Conference on Parsimony and Learning (Proceedings Track)*, 2024.

Tianyi Zhang, Varsha Kishore, Felix Wu, Kilian Q Weinberger, and Yoav Artzi. Bertscore: Evaluating text generation with bert. In *International Conference on Learning Representations*, 2020.

Xingxuan Zhang, Jiansheng Li, Wenjing Chu, Junjia Hai, Renzhe Xu, Yuqing Yang, Shikai Guan, Jiazheng Xu, and Peng Cui. On the out-of-distribution generalization of multimodal large language models. *arXiv preprint arXiv:2402.06599*, 2024a.

Yuhui Zhang, Alyssa Unell, Xiaohan Wang, Dhruba Ghosh, Yuchang Su, Ludwig Schmidt, and Serena Yeung-Levy. Why are visually-grounded language models bad at image classification? *Conference on Neural Information Processing Systems (NeurIPS)*, 2024b.

Lianmin Zheng, Wei-Lin Chiang, Ying Sheng, Siyuan Zhuang, Zhanghao Wu, Yonghao Zhuang, Zi Lin, Zhuohan Li, Dacheng Li, Eric Xing, et al. Judging llm-as-a-judge with mt-bench and chatbot arena. *Advances in Neural Information Processing Systems*, 36:46595–46623, 2023.

Guanglin Zhou, Zhongyi Han, Shiming Chen, Biwei Huang, Liming Zhu, Salman Khan, Xin Gao, and Lina Yao. Adapting large multimodal models to distribution shifts: The role of in-context learning. *arXiv preprint arXiv:2405.12217*, 2024.

Deyao Zhu, Jun Chen, Xiaoqian Shen, Xiang Li, and Mohamed Elhoseiny. MiniGPT-4: Enhancing vision-language understanding with advanced large language models. In *The Twelfth International Conference on Learning Representations*, 2024.

# Understanding Multimodal LLMs Under Distribution Shifts: An Information-Theoretic Approach
—Appendix—

## CONTENTS



## A RELATED WORKS

**Foundation models under distribution shifts.** Recent findings imply that fine-tuning on a relatively small amount of ID datasets hurts the OOD generalization capability of foundation models Kumar et al. (2022); Wortsman et al. (2022). Although lots of follow-up studies Goyal et al. (2023); Tian et al. (2023); Oh et al. (2025b) including theory-inspired methods Kumar et al. (2022); Ju et al. (2022); Oh et al. (2025a) have been proposed, almost all of them focused on a discriminative model such as CLIP Radford et al. (2021) for the image classification task. Given the rapidly growing popularity of MLLMs, it is necessary to investigate the reliability of MLLMs under distribution shifts with a tangible formulation. We lay a cornerstone for this.

**Performance analysis of MLLM.** There have been numerous reports on MLLMs' corner-case behaviors. Zhang et al. (2024a), Zhou et al. (2024), and Verma et al. (2024) observed that MLLMs poorly perform under specialized domains or synthetic perturbation, while Zhai et al. (2024) and Zhang et al. (2024b) showed that MLLMs are bad at some simple image classification tasks. Besides, Li et al. (2023b) and Ye-Bin et al. (2025) focused on the object hallucination of MLLM under spurious correlation. However, they all lacked a formal framework to explain such degradation of MLLMs. We recast the degeneration of MLLMs via robustness under distribution shifts between instruction-tuning and evaluation data Liang et al. (2025), and devise the first theoretical framework to analyze MLLMs.

**Information-theoretic approach for model evaluation.** As well as learning objectives Alemi et al. (2016); Chen et al. (2016); Tschannen et al. (2020); Kong et al. (2020); Wang et al. (2021), information-theoretic view has been steadily adopted to establish evaluation criteria for language model probing Hewitt et al. (2021), prompt engineering Sorensen et al. (2022), and rationale evaluation Chen et al. (2023), but relatively unexplored for MLLM yet. We also note some works adopting information-theoretic approaches to analyze models under distribution shifts Federici et al. (2021); Shui et al. (2022). Although they focused on classification tasks with discriminative models, we established new theorems for MLLM analysis based on our new metric, EMI.

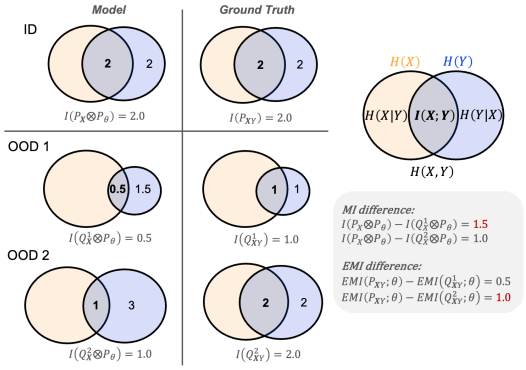


Figure 4: **Information diagram and motivation of effective mutual information.** The difference between vanilla MI terms does not consider the domain-dependent intrinsic scale and mutual information, thereby failing to fairly measure the relevance between input query $x$ and model prediction $\hat{y}$. Meanwhile, EMI ablates the domain-dependent characteristic to focus on measuring effective relevance between $x$ and $\hat{y}$.

## B Additional Description for Effective Mutual Information

We propose effective mutual information (EMI) as an alternative to vanilla mutual information (MI) to evaluate a model-generated output response given an input query. As explained in Section 4.2, MI (e.g., $I(P_{\mathbf{X}} \otimes P_\theta)$) can not take into account the intrinsic characteristics of data distribution. See Figure 4 for an intuitive example. The amount of information represented by entropy $H(\cdot)$ and conditional entropy $H(\cdot|\cdot)$ can vary depending on the data-generating process of each dataset. For example, if the task we are interested in is closer to solving a narrow problem in some specific domain (e.g., OOD1: LLaVA-Med; Li et al. (2024)), the cardinality of the desired output response space may be significantly smaller than that of a general problem-solving task in a general domain (e.g., OOD2: LLaVA-Bench Wild; Liu et al. (2023)), and the ground truth MI can differ depending on the domain. By considering these baseline amounts of information, EMI can measure how much our model captures **effective relevance** between input and output.

In Section 4.2, we provide some justifications for using EMI as an evaluation metric of MLLMs by revealing analogies to excess risk and effective robustness and presenting its theoretical connection to win rate. While LLM-as-a-Judge enables flexible evaluation for open-ended generation tasks with multiple user-defined criteria, EMI confines the facet of evaluation to query-response relevance. However, compromise in the flexibility of evaluation endows us to build solid theoretical statements that are necessary for understanding MLLMs and improving them in a principled way.

Meanwhile, as we adopt neural network models for empirical estimation of EMI, it is somewhat similar to the model-based heuristic metrics, such as BERTscore Zhang et al. (2020), BARTscore Yuan et al. (2021), and CLIPscore Hessel et al. (2021), that map input(s) to a scalar score through a single forward evaluation of the model. However, we take a step further beyond the simple working-heuristic method and lay a theoretical foundation with EMI.

## C Implementation Details

In this paper, we proposed EMI for a reliable evaluation of multimodal large language models (MLLMs) with a theoretical ground. Based on EMI, to analyze the MLLM performance gap under distribution shift, we provided the upper bound for EMI difference between ID and OOD data. In this section, we describe the procedures for estimating EMI and its upper bound in detail.

**Overview.** To estimate EMI and its upper bound, we first need to define estimators for MI and Jensen-Shannon divergence (JSD). Those estimators commonly adopt neural network encoders to project the raw data such as text and image into embedding space of neural networks to reduce problem complexity Oord et al. (2018); Liu et al. (2020), and then, MI estimator commonly optimizes a simple critic function Poole et al. (2019) on top of the embeddings of data. After training of MI

estimator, we evaluate empirical MI over different data distributions. For JSD estimation, given the embedding spaces of pre-trained models, additional training is not necessary. Therefore, the procedures can be divided into two phases: (1) neural MI estimator training, and (2) inference of MI and JSD.

**MI estimation.** Estimating MI with finite samples from unknown population distribution is a non-trivial problem, and has been actively studied Fraser & Swinney (1986); Paninski (2003); Kraskov et al. (2004); Nguyen et al. (2010); Shwartz-Ziv & Tishby (2017); Belghazi et al. (2018); Poole et al. (2019); Cheng et al. (2020). We adopted the contrastive log-ratio upper bound (CLUB; Cheng et al. (2020)) as our default MI estimator similar to Cheng et al. (2021). We first extract embeddings for visual input query $Z_v = \text{enc}_v(X_v)$ and text input query $Z_t = \text{enc}_t(X_t)$ from visual and text encoder models and take the mean of them to provide input query embedding $Z_{\mathbf{X}} = \frac{Z_v + Z_t}{2}$. Specifically, we adopt the most representative embedding models for each modality, i.e., CLIP pre-trained[1] ViT-B/32 and XLM-RoBERTa-Base[2] Conneau (2019) as visual and text encoders, respectively by default. We also obtain the embedding vectors for the model response $Z_{\hat{Y}} = \text{enc}_t(\hat{Y})$ and reference response $Z_Y = \text{enc}_t(Y)$ with text encoder model. Then, we train the MI estimator $\hat{I}_\psi(\cdot, \cdot)$ with parameter $\psi$ via gradient descent. To be specific, CLUB formulates the unbiased estimation for MI as below,

$$\hat{I}_{\text{CLUB}}(P_{Z_{\mathbf{X}} Z_Y}) = \frac{1}{N} \sum_{i=1}^{N} \log q_\psi(z_{y_i} | z_{x_i}) - \frac{1}{N^2} \sum_{i=1}^{N} \sum_{j=1}^{N} \log q_\psi(z_{y_j} | z_{x_i}), \tag{9}$$

where $q_\psi(\cdot|\cdot)$ denotes variational approximation of ground truth probability density function $p(\cdot|\cdot)$.

Following Cheng et al. (2020; 2021), we parameterize the $q_\psi$ as a multi-variate Gaussian distribution and estimate the mean and variance parameters of Gaussian with separated two-layer MLPs with 250 hidden dimension size. During mini-batch training, those MLPs consume the concatenated input and response embeddings $\{[z_{\mathbf{x}_i}, z_{y_i}]\}_{i=1}^N$ to produce a scalar estimate of MI, and they are simultaneously optimized by AdamW optimizer with learning rate 0.001 and batch size 1,024 for 5,000 iterations. However, if we have to train an estimator for every ID-OOD data pair, it may not be practical when the number of data pairs to be evaluated is large. Therefore, we constructed a dataset that integrates all ID-OOD data subsets for MI training (integration of all variants of LLaVA-Bench datasets reach roughly 5,000 samples for natural shift, and 9,000 samples for synthetic shift), trains it only once, and then infers all ID-OOD scenarios (27 for natural shift, 34 for synthetic shift) using this common MI estimator. This not only significantly reduces the time required to evaluate the model's robustness against multiple distribution shift scenarios, but also stabilizes the training process by increasing the size of the data set used in the training process.

**JS divergence estimation.** Estimation of distribution divergences from finite samples has been also a central topic of research Yang & Barron (1999); Sriperumbudur et al. (2012); Li & Turner (2016); Bu et al. (2018); Sinn & Rawat (2018); Sreekumar & Goldfeld (2022); Hoyos-Osorio & Sanchez-Giraldo (2023). We adopt the most recent one, representation Jensen-Shannon divergence (RJSD; Hoyos-Osorio & Sanchez-Giraldo (2023); Hoyos & Giraldo (2024)), which proves its effectiveness on real benchmark datasets as our JSD estimator. The formula is as follows:

$$\hat{D}_{\text{RJSD}}(P, Q) = S(\frac{C_P + C_Q}{2}) - \frac{1}{2}(S(C_P) + S(C_Q)), \tag{10}$$

where $C_P = \mathbb{E}_{X \sim P}[\phi(X) \otimes \phi(X)]$ and $S(C_P) = -\text{Trace}(C_P \log C_P)$. Similar to MI, we compute $\hat{D}_{\text{RJSD}}(P, Q)$ in the embedding space of the same frozen pre-trained models, i.e., leverage neural network embedding space as a kernel $< \phi(x), \phi(x') >$. In contrast to the case of MI, RJSD with a frozen neural embedding model does not require additional training. Still, one might consider learning the embedding model from scratch if necessary.

**MLLM judge and win rate.** For the open-ended generation tasks, (M)LLM-as-a-Judge has been adopted as a current de facto standard. Following Liu et al. (2023; 2024a), we use GPT-4[3] with

[1] `https://github.com/openai/CLIP`.

[2] `https://huggingface.co/FacebookAI/xlm-roberta-base`

[3] `gpt-4-turbo` with `2024-08-01-preview` API version was adopted

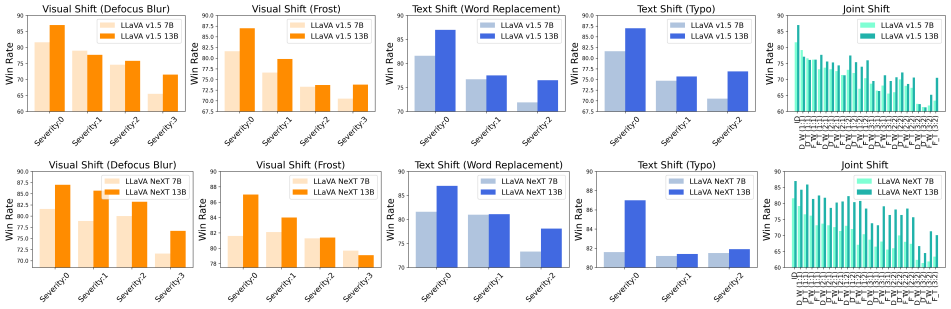


Figure 5: **Performance variation against varying degrees of distribution shifts.** We evaluated LLaVA v1.5 and LLaVA NeXT models on 34 out-of-distribution (OOD) variants induced by image and text perturbations of the LLaVA-Bench COCO dataset (ID). Here, the $x$-axis is sorted by the severity of shifts between ID and OOD. There is a consistent trend – increased degrees of distribution shifts result in performance degradations of MLLM.

text-only inference mode (with plain-text form visual cue such as ground truth caption for image) as a judge model and also use the output of the same model as a reference answer for each query. We leverage the prompts provided by the source code of LLaVA[4], and compute the win rate of a model of interest by comparing its output with that of GPT-4.

# D Extended Empirical Validation and Discussion

## D.1 Additional Result from Pilot Study

In Section 3, we conduct an experiment to validate our hypotheses on the relation between MLLM performance degradation and the severity of natural distribution shift. In Figure 5, we provide additional results from another type of distribution shift that occurred by image and text perturbations. For image perturbation, we consider defocus blur and frost with three different magnitudes, and for text perturbation, we consider keyboard typo error and word synonym replacement with two different magnitudes. We observe the consistent trend in the relation between MLLM performance degradation and the severity of distribution shifts for the case of visual-only, text-only, and joint shift, likewise the case of natural shifts in Figure 2. That is, the increased magnitude of distribution shifts induces more severe MLLM performance degradation, and the degree of performance degradation can attribute to shifts in two modalities.

## D.2 Partial bound analysis.

It is common that we can not access the ground truth response $Y$ from our evaluation dataset in advance. Then, one may want to use the EMID upper bound as an estimator of the maximum risk of MLLM given two datasets, i.e., $\max \text{EMID}(P_{\mathbf{X}Y}, Q_{\mathbf{X}Y}; \theta)$, by neglecting the output-related term $\Delta$. In Figure 6, we investigate whether the summation of two JS divergence terms can still be predictive for EMID. Although the trends become loose compared to the full bound due to the non-optimality of MLLM parameters, the partial upper bound still has moderate correlations (denoted by Pearson $r$) with EMID.

## D.3 Different Design Choices of MI and JSD Estimation

Note that the results of all theorem (Lemma 4.2, Theorem **??**, Theorem 4.3, and Theorem 4.4) are not limited to a specific class of MI and JSD estimators. To investigate whether our empirical verification of theorems robustly holds in an estimator-agnostic manner (if the estimator is valid), we provide an ablation study for the MI estimator, JSD estimator, and embedding space that the estimators are built on.

[4]https://github.com/haotian-liu/LLaVA

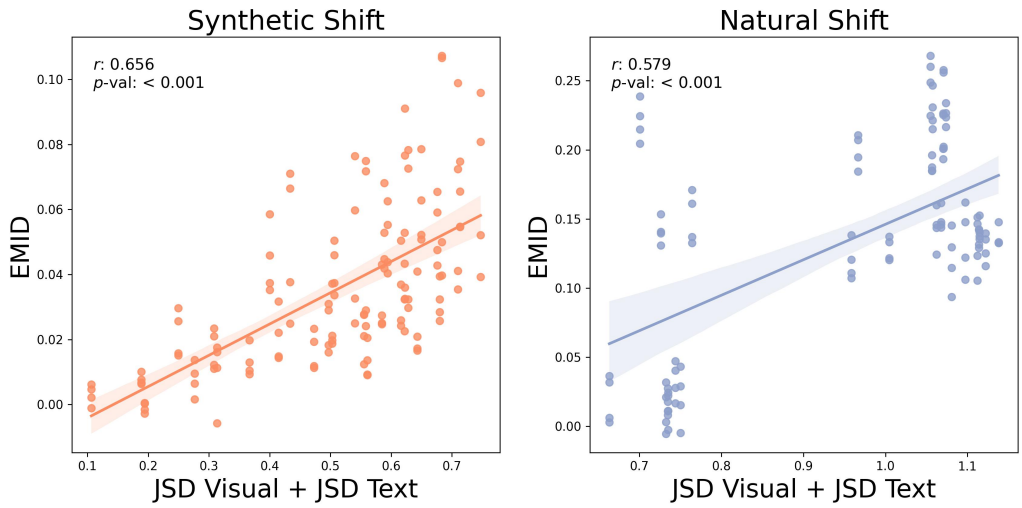


Figure 6: **Scatter plot with regression line between empirical estimates of EMID and partial components of its upper bound.** We remove the $\Delta$ term of bound (Eq. equation 8) and only use the estimates of JSD terms over visual and text inputs.

Specifically, we consider four MI estimators {NWJ Nguyen et al. (2010), MINE Belghazi et al. (2018), InfoNCE Oord et al. (2018), CLUB Cheng et al. (2020)}, three embedding spaces {individual models (CLIP ViT and XLM-RoBERTa), E5-V joint Jiang et al. (2024), E5-V disjoint Jiang et al. (2024)}, and two JSD estimators {MMD Liu et al. (2020), RJSDHoyos-Osorio & Sanchez-Giraldo (2023)}. E5-V Jiang et al. (2024) is a recently proposed embedding extraction method that leverages an MLLM with a carefully designed prompt. We used the default prompt "`Summary above sentence/image in one word: `" to separately extract embeddings (E5-V disjoint) for images and sentences, and design an ensemble of four custom prompts,

1. "`Summary of the image <image>, and sentence <sent> in one word: `"
2. "`Summary of the visual content "<image>" with an associated text query "<sent>" in one word: `"
3. "`Given <image>, Summary of the sentence "<sent>" in one word: `"
4. "`Given visual content "<image>", Summary of the text query "<sent>" in one word: `",

to extract multimodal joint query embedding (E5-V joint) by averaging four embedding vectors per (image, sentence) pair.

In Table 4, we conduct Spearman correlation analysis over the 12 ($4 \times 3$) cases of MI estimator and embedding space ablation. We can clearly see that EMI is consistently correlated with the win rate which demonstrates the robust effectiveness of our theorem in practice. Meanwhile, among the candidate MI estimators and embedding space, CLUB and two E5-V joint embeddings show outstanding results. However, E5-V embedding extraction require a forward pass of MLLM in contrast to the case of leveraging relatively small individual models (ViT base and BERT-base). To strike the balance between effectiveness and efficiency, we adopt CLIP ViT-B/32 and XLM-RoBERTa-Base embedding spaces by default.

Next, we present the Pearson correlation analysis result in Table 5 by ablating the JSD estimator with the MI estimator and embedding space choices. Although there are some variations in the exact values, we also observe consistently significant correlations between EMID and its upper bound (that of Theorem 8). Therefore, the upper bound of EMID we derived robustly holds in practice across diverse estimator configurations.

Table 4: **Ablation study for MI estimator and embedding space**. We evaluate four MI estimators with three different embedding space choices in terms of Spearman correlation coefficient $\rho$ between win rate and EMI. We can see that EMI and win rate are robustly correlated to variations in the embedding space and the MI estimator, but CLUB shows the most stable correlation.

| Configuration | | LLaVA v1.5 7B | | LLaVA v1.5 13B | | LLaVA NeXT 7B | | LLaVA NeXT 13B | |
|---|---|---|---|---|---|---|---|---|---|
| MI estimator | Embedding | $\rho$ | $p$-val | $\rho$ | $p$-val | $\rho$ | $p$-val | $\rho$ | $p$-val |
| CLUB | E5-V disjoint | 0.695 | 0.000 | 0.726 | 0.000 | 0.581 | 0.001 | 0.579 | 0.001 |
| CLUB | E5-V joint | 0.910 | 0.000 | 0.846 | 0.000 | 0.817 | 0.000 | 0.902 | 0.000 |
| CLUB | Individual models | 0.606 | 0.001 | 0.720 | 0.000 | 0.594 | 0.001 | 0.457 | 0.014 |
| InfoNCE | E5-V disjoint | 0.670 | 0.000 | 0.708 | 0.000 | 0.638 | 0.000 | 0.590 | 0.001 |
| InfoNCE | E5-V joint | 0.800 | 0.000 | 0.717 | 0.000 | 0.636 | 0.000 | 0.609 | 0.001 |
| InfoNCE | Individual models | 0.519 | 0.005 | 0.421 | 0.026 | 0.410 | 0.030 | 0.275 | 0.157 |
| MINE | E5-V disjoint | 0.664 | 0.000 | 0.605 | 0.001 | 0.269 | 0.167 | 0.278 | 0.153 |
| MINE | E5-V joint | 0.632 | 0.000 | 0.559 | 0.002 | 0.610 | 0.001 | 0.308 | 0.111 |
| MINE | Individual models | 0.632 | 0.000 | 0.562 | 0.002 | 0.632 | 0.000 | 0.613 | 0.001 |
| NWJ | E5-V disjoint | 0.583 | 0.001 | 0.552 | 0.002 | 0.513 | 0.005 | 0.429 | 0.023 |
| NWJ | E5-V joint | 0.502 | 0.005 | 0.519 | 0.005 | 0.492 | 0.008 | 0.480 | 0.010 |
| NWJ | Individual models | 0.510 | 0.006 | 0.717 | 0.000 | 0.488 | 0.008 | 0.322 | 0.095 |

Table 5: **Ablation study for MI estimator, JSD estimator, and embedding space**. We evaluate four MI estimator and two JSD estimator candidates, with three different embedding space choices in terms of Pearson correlation coefficient between EMID and its upper bound. In all the considered variations, EMID and the upper bound of EMID (i.e., the simplified version in Theorem 4.3) show strong correlations, implying that our theorem empirical robustly holds in practice.

| Configuration | | | Pearson | |
|---|---|---|---|---|
| JSD estimator | MI estimator | Embedding | $r$ | $p$-val |
| RJSD | CLUB | E5-V disjoint | 0.618 | 0.000 |
| RJSD | CLUB | E5-V joint | 0.659 | 0.000 |
| RJSD | CLUB | Individual models | 0.565 | 0.000 |
| RJSD | InfoNCE | E5-V disjoint | 0.618 | 0.000 |
| RJSD | InfoNCE | E5-V joint | 0.617 | 0.000 |
| RJSD | InfoNCE | Individual models | 0.295 | 0.002 |
| RJSD | MINE | E5-V disjoint | 0.602 | 0.000 |
| RJSD | MINE | E5-V joint | 0.534 | 0.000 |
| RJSD | MINE | Individual models | 0.630 | 0.000 |
| RJSD | NWJ | E5-V disjoint | 0.611 | 0.000 |
| RJSD | NWJ | E5-V joint | 0.413 | 0.000 |
| RJSD | NWJ | Individual models | 0.468 | 0.000 |
| MMD | CLUB | E5-V disjoint | 0.618 | 0.000 |
| MMD | CLUB | E5-V joint | 0.659 | 0.000 |
| MMD | CLUB | Individual models | 0.478 | 0.000 |
| MMD | InfoNCE | E5-V disjoint | 0.432 | 0.000 |
| MMD | InfoNCE | E5-V joint | 0.617 | 0.000 |
| MMD | InfoNCE | Individual models | 0.295 | 0.002 |
| MMD | MINE | E5-V disjoint | 0.602 | 0.000 |
| MMD | MINE | E5-V joint | 0.623 | 0.000 |
| MMD | MINE | Individual models | 0.630 | 0.000 |
| MMD | NWJ | E5-V disjoint | 0.611 | 0.000 |
| MMD | NWJ | E5-V joint | 0.273 | 0.004 |
| MMD | NWJ | Individual models | 0.468 | 0.000 |

### D.4 Hyperparameter Sensitivity

We provide the hyperparameter configuration for MI estimator training (Table 6) and further provide sensitivity analysis for varying hyperparameters (Figure 7). We see that the CLUB estimator is quite

robust to varying hyperparameters, i.e., batch size, learning rate, and hidden dimension, which implies the effectiveness of EMI estimation without intensive hyperparameter tuning.

Table 6: **Hyperparameter tuning grid and selected value for MI estimator training.** The hyperparameters are selected based on the variance of last 10 iterations during training.

| Parameter | Selected | Sweep |
|---|---|---|
| learning rate | 0.001 | {0.005, 0.001, 0.0005, 0.0001} |
| batch size | 1024 | {64, 128, 256, 512, 1024, 2048} |
| hidden dimension | 100/500 | {250, 500, 1000, 2000} |

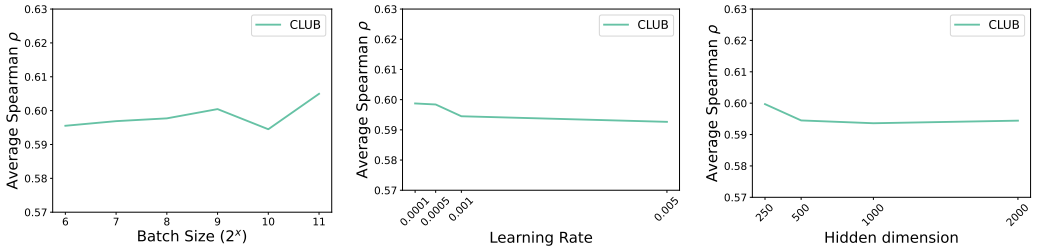


Figure 7: **Sensitivity analysis for batch size, learning rate, and hidden dimension during MI estimator training.** For the considered hyperparameter searching grid, MI estimates derived by the CLUB estimator robustly achieve high Spearman correlation with win rate (the largest deviation is less than 0.02 absolute value).

### D.5 Runtime Analysis

In addition to the advantage of allowing rigorous theoretical statements, EMI also has practical advantages over the win rate derived by the LLM judge. Specifically, while both win rate and EMI are model-dependent, the former relies on models with tens to hundreds of billions of parameters, while the latter enables meaningful evaluation even with relatively small embedding models with millions of parameters. To quantitatively argue this, we compare the time per instance and the total inference time for the entire LLaVA-Bench COCO dataset in Table 7. As shown in the table, EMI can shorten the time by 138 times compared to the win rate. Even including the time required for MI training, EMI-based evaluation is still 3 times faster than MLLM judgment-based evaluation. Since MI training is performed only once and then transferred to all ID-OOD scenarios, the efficiency of EMI-based evaluation over MLLM judgment becomes more evident as the number of datasets to be evaluated increases. In addition, in the LLM judge paradigm, although open-source LLM judges Kim et al. (2024) have been actively studied recently, proprietary LLMs are still dominant in practice, so one must pay per instance query, whereas EMI can make meaningful inferences with publicly available open-source pre-trained models without paying per query.

Table 7: **Runtime comparison on LLaVA-Bench COCO 90 samples.** We compare the actual wall-clock time (second) of EMI estimation and MLLM judgment protocols by evaluating model-generated response and reference response given input query from the LLaVA-Bench COCO dataset Liu et al. (2023). EMI estimation protocol on top of CLIP ViT-B/32 and XLM-RoBERTa-Base embedding achieves 138 times boosting from MLLM judgment protocol with GPT-4o.

| | LLaVA v1.5 7B | | LLaVA v1.5 13B | | LLaVA NeXT 7B | | LLaVA NeXT 13B | | Total runtime |
|---|---|---|---|---|---|---|---|---|---|
| | per instance | dataset | per instance | dataset | per instance | dataset | per instance | dataset | |
| MI estimator training | 663.45 | | | | | | | | 663.45 |
| EMI estimation | 0.0388 | 3.5884 | 0.0392 | 3.5652 | 0.0412 | 3.7107 | 0.0411 | 3.7039 | 14.56 (× 138 boosting) |
| MLLM judgment (GPT-4o API) | 5.49 | 493.75 | 5.48 | 493.59 | 5.52 | 496.66 | 5.83 | 524.45 | 2008.45 |

# E PROOF AND ADDITIONAL THEOREM

In this section, we provide proof of all theorems (Lemma 4.2, Theorem **??**, Theorem 4.3, and Theorem 4.4) in our manuscript, and introduce an additional theoretical result (Corollary E.12).

## E.1 PROOF FOR THE RELATIONSHIP BETWEEN EMI AND PREFERENCE MODEL

First, we provide proof of the closeness between the effective mutual information (EMI) and the preference model.

**Lemma E.1 (Restatment of Lemma 4.2)** *Given a distribution $P_{\mathbf{X}Y}$ and an MLLM $P_\theta$, let the reward model function $r(\mathbf{x}, y)$ be $\log P_{Y|\mathbf{X}=\mathbf{x}}(y)$. If $\mathbb{E}_{\mathbf{x}\sim P_\mathbf{X}} D_{\mathrm{KL}}(P_\theta(\cdot|\mathbf{x})\|P_{Y|\mathbf{X}=\mathbf{x}}) \le \delta$, then,*

$$|\textit{EMI}(P_{\mathbf{X}Y};\theta) - \textit{PM}(P_{\mathbf{X}Y};\theta)| \le \delta + 4.4\delta^{\frac{1}{8}}.$$

Let $P_{Y_\theta} = \mathbb{E}_{\mathbf{x}\sim\mathbf{X}} P_\theta(\cdot|\mathbf{x})$, and note the expression for EMI below,

$$\begin{aligned}
\mathrm{EMI}(P_{\mathbf{X}Y};\theta) &= I(P_\mathbf{X} \otimes P_\theta) - I(P_{\mathbf{X}Y}) \\
&= H(P_{Y_\theta}) - H(P_\theta(\cdot|\mathbf{X})) - H(P_Y) + H(P_{Y|\mathbf{X}}) \\
&= \big(H(P_{Y_\theta}) - H(P_Y)\big) \\
&+ \mathbb{E}_{\mathbf{x}\sim P_\mathbf{X}}[\mathbb{E}_{\hat{y}\sim P_\theta(\cdot|\mathbf{x})} \log P_\theta(\hat{y}|\mathbf{x})] - \mathbb{E}_{\mathbf{x}\sim P_\mathbf{X}}[\mathbb{E}_{y\sim P_{Y|\mathbf{X}=\mathbf{x}}} \log P_{Y|\mathbf{X}=\mathbf{x}}(y)]
\end{aligned}$$

Next, given $r(\mathbf{x}, y) = \log P_{Y|\mathbf{X}=\mathbf{x}}(y)$, logit Bradley-Terry preference model (PM) Hunter (2004) can be expressed as,

$$\mathrm{PM}(P_{\mathbf{X}Y};\theta) = \mathbb{E}_{\mathbf{x}\sim P_\mathbf{X}}[\mathbb{E}_{\hat{y}\sim P_\theta(\cdot|\mathbf{x})} \log P_{Y|\mathbf{X}=\mathbf{x}}(\hat{y}) - \mathbb{E}_{y\sim P_{Y|\mathbf{X}=\mathbf{x}}} \log P_{Y|\mathbf{X}=\mathbf{x}}(y)]$$

Therefore,

$$\begin{aligned}
|\mathrm{EMI}(P_{\mathbf{X}Y};\theta) - \mathrm{PM}(P_{\mathbf{X}Y};\theta)| &= |H(P_{Y_\theta}) - H(P_Y) + \mathbb{E}_{\mathbf{x}\sim P_\mathbf{X}}[\mathbb{E}_{\hat{y}\sim P_\theta(\cdot|\mathbf{x})} \log \frac{P_\theta(\hat{y}|\mathbf{x})}{P_{Y|\mathbf{X}=\mathbf{x}}(\hat{y})}]| \\
&\le |H(P_{Y_\theta}) - H(P_Y)| + \mathbb{E}_{\mathbf{x}\sim P_\mathbf{X}}[D_{\mathrm{KL}}(P_\theta(\cdot|\mathbf{x})||P_{Y|\mathbf{X}=\mathbf{x}})] \\
&\le 4.4\delta^{\frac{1}{8}} + \delta.
\end{aligned}$$

Here, we adopted Lemma E.4 to replace $|H(P_{Y_\theta}) - H(P_Y)|$ into its upper bound $4D_{\mathrm{JS}}^{\frac{1}{4}}(P_{Y_\theta}||P_Y)$ and used Pinsker's inequality Pinsker (1964).

We provide a proof for the extended theorem from the Lemma E.2 by considering the optimal model parameter as below.

**Theorem E.2** *Given a distribution $P_{\mathbf{X}Y}$ and an MLLM $P_\theta$, and assume $P_{\mathbf{X}Y} > c > 0$ for a constant $c$, if the $\epsilon$-representation capacity assumption holds, i.e.,*

$$\min_{\theta\in\Theta} \mathbb{E}_{\mathbf{x}\sim P_\mathbf{X}} D_{\mathrm{KL}}(P_{Y|\mathbf{X}=\mathbf{x}}\|P_\theta(\cdot|\mathbf{x})) \le \epsilon, \tag{11}$$

*and let the reward function $r(\mathbf{x}, y)$ be $\log P_{Y|\mathbf{X}=\mathbf{x}}(y)$, then*

$$|\textit{EMI}(P_{\mathbf{X}Y};\theta^*) - \textit{PM}(P_{\mathbf{X}Y};\theta^*)| \le \delta + 4.4\delta^{\frac{1}{8}},$$

*where $\theta^*$ is the optimal solution of Eq. 1 over $P_{\mathbf{X}Y}$, and $\delta = 4.4\epsilon^{\frac{1}{8}} - \log c\sqrt{2\epsilon}$.*

Theorem E.2 shows that with a sufficiently expressive model class, EMI exhibits a stronger alignment with PM when the optimal MLLM parameter $\theta^*$ is obtained through the autoregressive objective. This alignment underscores the validity of using EMI as a reliable metric for evaluating MLLM and quantifying the relative preference of responses. Recall the formulation of mutual information as below,

$$\begin{aligned}
I(P_{\mathbf{X}Y}) &= H(P_Y) - H(P_{Y|\mathbf{X}}) \\
&= \mathbb{E}_{\mathbf{x},y\sim P_{\mathbf{X}Y}}[\log P_{Y|X=x}(y)] + H(P_Y) \\
&= \mathbb{E}_{\mathbf{x},y\sim P_{\mathbf{X}Y}}[\log P_\theta(y|\mathbf{x})] - \mathbb{E}_{\mathbf{x},y\sim P_{\mathbf{X}Y}}[\log P_\theta(y|\mathbf{x})] + \mathbb{E}_{\mathbf{x},y\sim P_{\mathbf{X}Y}}[\log P_{Y|X=x}(y)] + H(P_Y) \\
&= \mathbb{E}_{\mathbf{x},y\sim P_{\mathbf{X}Y}}[\log P_\theta(y|\mathbf{x})] + \mathbb{E}_{\mathbf{x}\sim P_\mathbf{X}}[D_{\mathrm{KL}}(P_{Y|\mathbf{X}=\mathbf{x}}||P_\theta(\cdot|\mathbf{x}))] + H(P_Y)
\end{aligned}$$

So, $I(P_{\mathbf{X}Y}) - \mathbb{E}_{\mathbf{x},y\sim P_{\mathbf{X}Y}}[\log P_\theta(y|\mathbf{x})] - H(P_Y) = \mathbb{E}_{\mathbf{x}\sim P_{\mathbf{X}}}[D_{\mathrm{KL}}(P_{Y|\mathbf{X}=x}(y)||P_\theta(\cdot|\mathbf{x}))]$. Therefore, for the optimally learned parameter $\theta^*$, we know that $\theta^* \in \arg\min_{\theta\in\Theta} \mathbb{E}_{\mathbf{x}\sim P_{\mathbf{X}}}[D_{\mathrm{KL}}(P_{Y|\mathbf{X}=\mathbf{x}}||P_\theta(\cdot|\mathbf{x}))]$, which implies below,

$$\mathbb{E}_{\mathbf{x}\sim P_{\mathbf{X}}}[D_{\mathrm{KL}}(P_{Y|\mathbf{X}=x}||P_{\theta^*}(\cdot|\mathbf{x}))] \leq \epsilon.$$

Meanwhile, we have the below upper bound by leveraging Lemma E.7,

$$\mathbb{E}_{\mathbf{x}\sim P_{\mathbf{X}}}[D_{\mathrm{KL}}(P_\theta(\cdot|\mathbf{x})||P_{Y|\mathbf{X}=\mathbf{x}})] \leq 4.4\epsilon^{\frac{1}{8}} - \log c\sqrt{2\epsilon}$$

By denoting $\delta := 4.4\epsilon^{\frac{1}{8}} - \log c\sqrt{2\epsilon}$ and plugging the Lemma E.1, we complete the proof.

Note that the assumption $P_{\mathbf{X}Y} > c > 0$ is reasonable in practice given the following two statements. First, we can only observe the samples that $P_{\mathbf{X}Y}(\mathbf{x}, y) > 0$. Therefore, investigating on the case $\mathbf{x}, y$ such that $P_{\mathbf{X}Y} > 0$ solely does not affect the practical implication of our analysis. Second, for the space $\mathcal{X} \times \mathcal{Y}$, it is obvious that $|\mathcal{X} \times \mathcal{Y}| < +\infty$. Therefore, $\mathcal{X} \times \mathcal{Y}$ is a compact space, and $P_{\mathbf{X}Y}(\mathbf{x}, y) > 0$ over a compact space, there exists a constant $c > 0$ such that $P_{\mathbf{X}Y}(\mathbf{x}, y) > c$.

**Lemma E.3** *Given two distributions $P_X$ and $Q_X$ defined over $\mathcal{X}$, let $f : \mathcal{X} \to [0, c]$, then we have the below,*

$$\left|\mathbb{E}_{x\sim P_X}[f(x)] - \mathbb{E}_{x\sim Q_X}[f(x)]\right| \leq c \cdot D_{\mathrm{TV}}(P_X, Q_X).$$

*where $D_{\mathrm{TV}}(P_X, Q_X) := \sum_{x\in X} |P_X(x) - Q_X(x)|$ is the total variation distance between two distributions.*

$$\begin{aligned}
&\left|\mathbb{E}_{x\sim P_X}[f(x)] - \mathbb{E}_{x\sim Q_X}[f(x)]\right| \\
=&\Big|\sum_{x\in\mathcal{X}} P_X(x)f(x) \sum_{x\in\mathcal{X}} Q_X(x)f(x)\Big| \\
=&\Big|\sum_{x\in\mathcal{X}} (P_X(x) - Q_X(x))f(x)\Big| \\
=&\Big|\sum_{x\in\mathcal{X}} (P_X(x) - Q_X(x))(f(x) - c) + c(\sum_{x\in\mathcal{X}} P_X(x) - Q_X(x))\Big| \\
\leq& \sum_{x\in\mathcal{X}} |P_X(x) - Q_X(x)| \cdot \left|f(x) - c\right| \\
\leq& c \cdot ||P_X - Q_X||_1 \\
=& c \cdot D_{\mathrm{TV}}(P_X, Q_X)
\end{aligned}$$

**Lemma E.4** *Given random variable $\mathbf{X}$, and two distributions $P_{\mathbf{X}Y} = P_{Y|\mathbf{X}}P_{\mathbf{X}}$ and $Q_{\mathbf{X}Y} = Q_{Y|\mathbf{X}}Q_{\mathbf{X}}$, we have the bounds for the difference between Entropy $H(\cdot)$ over two distributions as below:*

$$\begin{aligned}
|H(P_{\mathbf{X}}) - H(Q_{\mathbf{X}})| &\leq 4D_{\mathrm{JS}}^{\frac{1}{4}}(P_{\mathbf{X}}||Q_{\mathbf{X}}), \\
|H(P_Y) - H(Q_Y)| &\leq 4D_{\mathrm{JS}}^{\frac{1}{4}}(P_Y||Q_Y), \\
|H(P_{Y|\mathbf{X}=\mathbf{x}}) - H(Q_{Y|\mathbf{X}=\mathbf{x}})| &\leq 4D_{\mathrm{JS}}^{\frac{1}{4}}(P_{Y|\mathbf{X}=\mathbf{x}}||Q_{Y|\mathbf{X}=\mathbf{x}}).
\end{aligned}$$

*where $D_{\mathrm{JS}}(\cdot, \cdot)$ is the Jensen-Shannon divergence between two distributions.*

Let $M_{\mathbf{X}} = (P_{\mathbf{X}} + Q_{\mathbf{X}})/2$, $D_{\mathrm{JS}}(P_{\mathbf{X}}, Q_{\mathbf{X}})$ and $D_{\mathrm{TV}}(P_{\mathbf{X}}, Q_{\mathbf{X}})$ be the Jensen-Shannon divergence and total variation distance between $P_{\mathbf{X}}$ and $Q_{\mathbf{X}}$, respectively.

$$
\begin{aligned}
&\big|H(P_{\mathbf{X}}) - H(Q_{\mathbf{X}})\big| \\
=&\big|\mathbb{E}_{\mathbf{x}\sim P_{\mathbf{X}}} \log P_{\mathbf{X}}(\mathbf{x}) - \mathbb{E}_{\mathbf{x}\sim Q_{\mathbf{X}}} \log Q_{\mathbf{X}}(\mathbf{x})\big| \\
=&\big|\mathbb{E}_{\mathbf{x}\sim P_{\mathbf{X}}} \log P_{\mathbf{X}}(\mathbf{x}) - \mathbb{E}_{\mathbf{x}\sim P_{\mathbf{X}}} \log M_{\mathbf{X}}(\mathbf{x}) - \mathbb{E}_{\mathbf{x}\sim Q_{\mathbf{X}}} \log Q_{\mathbf{X}}(\mathbf{x}) + \mathbb{E}_{\mathbf{x}\sim Q_{\mathbf{X}}} \log M_{\mathbf{X}}(\mathbf{x}) + \mathbb{E}_{\mathbf{x}\sim P_{\mathbf{X}}} \log M_{\mathbf{X}}(\mathbf{x}) - \mathbb{E}_{\mathbf{x}\sim Q_{\mathbf{X}}} \log M_{\mathbf{X}}(\mathbf{x})\big| \\
\leq&|\mathbb{E}_{\mathbf{x}\sim P_{\mathbf{X}}} \log \frac{P_{\mathbf{X}}(\mathbf{x})}{M_{\mathbf{X}}(\mathbf{x})} - \mathbb{E}_{\mathbf{x}\sim Q_{\mathbf{X}}} \log \frac{Q_{\mathbf{X}}(\mathbf{x})}{M_{\mathbf{X}}(\mathbf{x})}| + |\mathbb{E}_{\mathbf{x}\sim P_{\mathbf{X}}} \log M_{\mathbf{X}}(\mathbf{x}) - \mathbb{E}_{\mathbf{x}\sim Q_{\mathbf{X}}} \log M_{\mathbf{X}}(\mathbf{x})| \\
\leq&|\mathbb{E}_{\mathbf{x}\sim P_{\mathbf{X}}} \log \frac{P_{\mathbf{X}}(\mathbf{x})}{M_{\mathbf{X}}(\mathbf{x})} + \mathbb{E}_{\mathbf{x}\sim Q_{\mathbf{X}}} \log \frac{Q_{\mathbf{X}}(\mathbf{x})}{M_{\mathbf{X}}(\mathbf{x})}| + |\mathbb{E}_{\mathbf{x}\sim P_{\mathbf{X}}} \log M_{\mathbf{X}}(\mathbf{x}) - \mathbb{E}_{\mathbf{x}\sim Q_{\mathbf{X}}} \log M_{\mathbf{X}}(\mathbf{x})| \\
\leq&2D_{\mathrm{JS}}(P_{\mathbf{X}}||Q_{\mathbf{X}}) + 2\sum_x |\frac{P_{\mathbf{X}}(x)}{2} - \frac{Q_{\mathbf{X}}(x)}{2}| \cdot |\log M_{\mathbf{X}}(x)| \\
=&2D_{\mathrm{JS}}(P_{\mathbf{X}}||Q_{\mathbf{X}}) + 2\sum_x |\frac{P_{\mathbf{X}}(x)}{2} - \frac{Q_{\mathbf{X}}(x)}{2}| \cdot \big|\log |\frac{P_{\mathbf{X}}(x)}{2} + \frac{Q_{\mathbf{X}}(x)}{2}|\big| \\
\leq&2D_{\mathrm{JS}}(P_{\mathbf{X}}||Q_{\mathbf{X}}) + 2\sum_x |\frac{P_{\mathbf{X}}(x)}{2} - \frac{Q_{\mathbf{X}}(x)}{2}| \cdot \big|\log |\frac{P_{\mathbf{X}}(x)}{2} - \frac{Q_{\mathbf{X}}(x)}{2}|\big| \\
\leq&2D_{\mathrm{JS}}(P_{\mathbf{X}}||Q_{\mathbf{X}}) + 2\sum_x \sqrt{|\frac{P_{\mathbf{X}}(x)}{2} - \frac{Q_{\mathbf{X}}(x)}{2}|} \\
\leq&2D_{\mathrm{JS}}(P_{\mathbf{X}}||Q_{\mathbf{X}}) + \sqrt{2\sum_x |P_{\mathbf{X}}(x) - Q_{\mathbf{X}}(x)|} \\
=&2D_{\mathrm{JS}}(P_{\mathbf{X}}||Q_{\mathbf{X}}) + \sqrt{2D_{\mathrm{TV}}(P_{\mathbf{X}}, Q_{\mathbf{X}})} \\
\leq&2D_{\mathrm{JS}}(P_{\mathbf{X}}||Q_{\mathbf{X}}) + 2D_{\mathrm{JS}}^{\frac{1}{4}}(P_{\mathbf{X}}||Q_{\mathbf{X}}) \\
\leq&4D_{\mathrm{JS}}^{\frac{1}{4}}(P_{\mathbf{X}}||Q_{\mathbf{X}})
\end{aligned}
$$

In above inequalities, we have used $\sqrt{x} + x\log x > 0$ for $x \in (0, 1)$, Holder's inequality, and $D_{\mathrm{TV}}(P_{\mathbf{X}}, Q_{\mathbf{X}}) \leq \sqrt{2D_{\mathrm{JS}}(P_{\mathbf{X}}\|Q_{\mathbf{X}})}$ proved in Lemma 3 of Thekumparampil et al. (2018). We can prove below with the same strategy,

$$
\begin{aligned}
|H(P_Y) - H(Q_Y)| &\leq 4D_{\mathrm{JS}}^{\frac{1}{4}}(P_Y||Q_Y), \\
|H(P_{Y|\mathbf{X}=\mathbf{x}}) - H(Q_{Y|\mathbf{X}=\mathbf{x}})| &\leq 4D_{\mathrm{JS}}^{\frac{1}{4}}(P_{Y|\mathbf{X}=\mathbf{x}}||Q_{Y|\mathbf{X}=\mathbf{x}}).
\end{aligned}
$$

**Corollary E.5** *For a data distribution $P_{\mathbf{X}Y} = P_{Y|\mathbf{X}}P_{\mathbf{X}}$, MLLM $P_\theta(\cdot|\mathbf{x})$, and Kullback-Leibler divergence $D_{\mathrm{KL}}$, if $\mathbb{E}_{\mathbf{x}\sim P_{\mathbf{X}}} D_{\mathrm{KL}}(P_{Y|\mathbf{X}=\mathbf{x}}\|P_\theta(\cdot|\mathbf{x}))) \leq \epsilon$ for a constant $\epsilon$, then*

$$
\mathbb{E}_{\mathbf{x}\sim P_{\mathbf{X}}}[H(P_\theta(\cdot|\mathbf{x})) - H(P_{Y|\mathbf{X}=\mathbf{x}})] \leq 4.4\epsilon^{\frac{1}{8}}
$$

$$
\begin{aligned}
\mathbb{E}_{\mathbf{x}\sim P_{\mathbf{X}}}[H(P_\theta(\cdot|\mathbf{x})) - H(P_{Y|\mathbf{X}=\mathbf{x}})] &\leq \mathbb{E}_{\mathbf{x}\sim P_{\mathbf{X}}}[\big|H(P_\theta(\cdot|\mathbf{x})) - H(P_{Y|\mathbf{X}=\mathbf{x}})\big|] \\
&\leq 4\mathbb{E}_{\mathbf{x}\sim P_{\mathbf{X}}} D_{\mathrm{JS}}^{\frac{1}{4}}(P_{Y|\mathbf{X}=\mathbf{x}}||P_\theta(\cdot|\mathbf{x})) \\
&\leq 4\cdot 2^{\frac{1}{8}}\mathbb{E}_{\mathbf{x}\sim P_{\mathbf{X}}} D_{\mathrm{KL}}^{\frac{1}{8}}(P_{Y|\mathbf{X}=\mathbf{x}}||P_\theta(\cdot|\mathbf{x})) \\
&\leq 4.4\epsilon^{\frac{1}{8}}.
\end{aligned}
$$

We started from Lemma E.4 and use Pinsker's inequality Pinsker (1964) to leverage $D_{\mathrm{JS}}(\cdot|\cdot) \leq D_{\mathrm{TV}}(\cdot,\cdot) \leq \sqrt{2D_{\mathrm{KL}}(\cdot|\cdot)}$.

**Lemma E.6** *For a data distribution $P_{\mathbf{X}Y} = P_{Y|\mathbf{X}}P_{\mathbf{X}}$, MLLM $P_\theta(\cdot|\mathbf{x})$, let $D_{\mathrm{KL}}$ and $D_{\mathrm{TV}}$ be Kullback-Leibler divergence and total variation distance, respectively. Denote $P_{Y_\theta} = \mathbb{E}_{\mathbf{x}\sim P_{\mathbf{X}}}[P_\theta(\cdot|\mathbf{x})]$, we have below inequality.*

$$
D_{\mathrm{TV}}(P_Y, P_{Y_\theta}) \leq \sqrt{2\mathbb{E}_{\mathbf{x}\sim P_{\mathbf{X}}} D_{\mathrm{KL}}(P_\theta(\cdot|\mathbf{x})||P_{Y|\mathbf{X}=\mathbf{x}})}.
$$

$$
\begin{aligned}
D_{\mathrm{TV}}(P_Y, P_{Y_\theta}) =& \sum_{y\in\mathcal{Y}} \left|\mathbb{E}_{\mathbf{x}\sim P_{\mathbf{X}}} P_{Y|\mathbf{X}=\mathbf{x}}(y) - \mathbb{E}_{\mathbf{x}\sim P_{\mathbf{X}}} P_\theta(y|\mathbf{x})\right| \\
\leq& \sum_{y\in\mathcal{Y}} \mathbb{E}_{\mathbf{x}\sim P_{\mathbf{X}}} \left|P_{Y|\mathbf{X}=\mathbf{x}}(y) - P_\theta(y|\mathbf{x})\right| \\
=& \mathbb{E}_{\mathbf{x}\sim P_{\mathbf{X}}} D_{\mathrm{TV}}(P_{Y|\mathbf{X}=\mathbf{x}}, P_\theta(\cdot|\mathbf{x})) \\
\leq& \sqrt{2\mathbb{E}_{\mathbf{x}\sim P_{\mathbf{X}}} D_{\mathrm{KL}}(P_\theta(\cdot|\mathbf{x})||P_{Y|\mathbf{X}=\mathbf{x}})}
\end{aligned}
$$

**Lemma E.7** *For a data distribution $P_{\mathbf{X}Y} = P_{Y|\mathbf{X}}P_{\mathbf{X}}$, MLLM $P_\theta(\cdot|\mathbf{x})$, and Kullback-Leibler divergence $D_{\mathrm{KL}}$, if $\mathbb{E}_{\mathbf{x}\sim P_{\mathbf{X}}} D_{\mathrm{KL}}(P_{Y|\mathbf{X}=\mathbf{x}}\|P_\theta(\cdot|\mathbf{x}))) \leq \epsilon$ and $P_{\mathbf{X}Y} > c > 0$ for a constant $c$ and $\epsilon$, then*

$$
\mathbb{E}_{\mathbf{x}\sim P_{\mathbf{X}}} D_{\mathrm{KL}}(P_\theta(\cdot|\mathbf{x}))\|P_{Y|\mathbf{X}=\mathbf{x}}) \leq 4.4\epsilon^{\frac{1}{8}} - \log c\sqrt{2\epsilon}.
$$

Note that

$$
\begin{aligned}
\mathbb{E}_{\mathbf{x}\sim P_{\mathbf{X}}}[H(P_\theta(\cdot|\mathbf{x})) - H(P_{Y|\mathbf{X}=\mathbf{x}})] =& \mathbb{E}_{\mathbf{x}\sim P_{\mathbf{X}}}[\mathbb{E}_{y\sim P_\theta(\cdot|\mathbf{x})} \log P_{Y|\mathbf{X}=\mathbf{x}}(y) - \mathbb{E}_{y\sim P_{Y|\mathbf{X}=\mathbf{x}}} \log P_{Y|\mathbf{X}=\mathbf{x}}(y)] \\
&+\mathbb{E}_{\mathbf{x}\sim P_{\mathbf{X}}} D_{\mathrm{KL}}(P_\theta(\cdot|\mathbf{x}))\|P_{Y|\mathbf{X}=\mathbf{x}}).
\end{aligned}
$$

Therefore,

$$
\begin{aligned}
\mathbb{E}_{\mathbf{x}\sim P_{\mathbf{X}}} D_{\mathrm{KL}}(P_\theta(\cdot|\mathbf{x}))\|P_{Y|\mathbf{X}=\mathbf{x}}) \leq& \left|\mathbb{E}_{\mathbf{x}\sim P_{\mathbf{X}}}[\mathbb{E}_{y\sim P_\theta(\cdot|\mathbf{x})} \log P_{Y|\mathbf{X}=\mathbf{x}}(y) - \mathbb{E}_{y\sim P_{Y|\mathbf{X}=\mathbf{x}}} \log P_{Y|\mathbf{X}=\mathbf{x}}(y)]\right| \\
&+ \mathbb{E}_{\mathbf{x}\sim P_{\mathbf{X}}}[H(P_\theta(\cdot|\mathbf{x})) - H(P_{Y|\mathbf{X}=\mathbf{x}})]
\end{aligned}
$$

Given Lemma E.3, it is easy to check that

$$
\begin{aligned}
&\left|\mathbb{E}_{\mathbf{x}\sim P_{\mathbf{X}}}[\mathbb{E}_{y\sim P_\theta(\cdot|\mathbf{x})} \log P_{Y|\mathbf{X}=\mathbf{x}}(y) - \mathbb{E}_{y\sim P_{Y|\mathbf{X}=\mathbf{x}}} \log P_{Y|\mathbf{X}=\mathbf{x}}(y)]\right| \\
\leq& -\log c\, \mathbb{E}_{\mathbf{x}\sim P_{\mathbf{X}}} D_{\mathrm{TV}}(P_\theta(\cdot|\mathbf{x}), P_{Y|\mathbf{X}=\mathbf{x}}) \\
\leq& -\log c\sqrt{2\epsilon}.
\end{aligned}
$$

Then, with Corollary E.5, we complete this proof.

### E.2 Proof for EMID upper bound

Now, we give the proof for the upper bound of the EMI Difference (EMID) as below.

**Theorem E.8 (General scenario)** *Given $P_{\mathbf{X}Y}$ and $Q_{\mathbf{X}Y}$ distributions and an MLLM $P_\theta$, if there exist some constants $\delta_P$ and $\delta_Q$ such that*

$$
D_{\mathrm{JS}}(P_{Y_\theta}\|P_Y) \leq \delta_P, \quad D_{\mathrm{JS}}(Q_{Y_\theta}\|Q_Y) \leq \delta_Q,
$$

*where $P_{Y_\theta} = \mathbb{E}_{\mathbf{x}\sim P_{\mathbf{X}}} P_\theta(\cdot|\mathbf{x})$ and $Q_{Y_\theta} = \mathbb{E}_{\mathbf{x}\sim Q_{\mathbf{X}}} P_\theta(\cdot|\mathbf{x})$, then EMID$(P_{\mathbf{X}Y}, Q_{\mathbf{X}Y}; \theta)$ is upper bounded by*

$$
\begin{aligned}
&\widehat{H}\big(D_{\mathrm{JS}}^{\frac{1}{2}}(P_{X_v}||Q_{X_v}) + D_{\mathrm{JS}}^{\frac{1}{2}}(P_{X_t}||Q_{X_t})\big) \\
+&\widehat{H}\big(\bar{D}_{\mathrm{JS}}^{\frac{1}{2}}(P_{X_t|X_v}\|Q_{X_t|X_v}) + \bar{D}_{\mathrm{JS}}^{\frac{1}{2}}(P_{X_v|X_t}\|Q_{X_v|X_t})\big) \\
+&4\mathbb{E}_{\mathbf{x}\sim P_{\mathbf{X}}}[D_{\mathrm{JS}}^{\frac{1}{4}}(P_{Y|\mathbf{X}=\mathbf{x}}\|Q_{Y|\mathbf{X}=\mathbf{x}})] + 8\Delta^{\frac{1}{4}},
\end{aligned}
$$

*where $\Delta = \delta_P + \delta_Q$, $\widehat{H} = \max_{\mathbf{x}\in\mathcal{X}}[H(Q_{Y|\mathbf{X}=\mathbf{x}}) + H(P_\theta(\cdot|\mathbf{x}))]$ and*
$\bar{D}_{\mathrm{JS}}(P_{X|X'}||Q_{X|X'}) := \mathbb{E}_{\mathbf{x}\sim P_{X'}} D_{\mathrm{JS}}(P_{X|X'=\mathbf{x}}\|Q_{X|X'=\mathbf{x}}) + \mathbb{E}_{\mathbf{x}\sim Q_{X'}} D_{\mathrm{JS}}(P_{X|X'=\mathbf{x}}\|Q_{X|X'=\mathbf{x}})$.

Let $P_{Y_\theta} = \mathbb{E}_{\mathbf{x}\sim P_{\mathbf{X}}} P_\theta(\cdot|\mathbf{x})$ and $Q_{Y_\theta} = \mathbb{E}_{\mathbf{x}\sim Q_{\mathbf{X}}} P_\theta(\cdot|\mathbf{x})$, EMID can be expressed with entropy and conditional entropy terms as below.

$$
\begin{aligned}
&\mathrm{EMID}(P_{\mathbf{X}Y}, Q_{\mathbf{X}Y}; \theta) \\
&= \mathrm{EMI}(P_{\mathbf{X}Y}; \theta) - \mathrm{EMI}(Q_{\mathbf{X}Y}; \theta) \\
&= (H(P_{Y_\theta}) - \mathbb{E}_{\mathbf{x}\sim P_{\mathbf{X}}}[H(P_\theta(\cdot|\mathbf{x}))] - H(P_Y) + H(P_{Y|\mathbf{X}})) - ((H(Q_{Y_\theta}) - \mathbb{E}_{\mathbf{x}\sim Q_{\mathbf{X}}}[H(P_\theta(\cdot|\mathbf{x}))] - H(Q_Y) + H(Q_{Y|\mathbf{X}})) \\
&\leq (H(P_{Y|\mathbf{X}}) - H(Q_{Y|\mathbf{X}})) + \big(\mathbb{E}_{\mathbf{x}\sim Q_{\mathbf{X}}}[H(P_\theta(\cdot|\mathbf{x}))] - \mathbb{E}_{\mathbf{x}\sim P_{\mathbf{X}}}[H(P_\theta(\cdot|\mathbf{x}))]\big) + |H(P_{Y_\theta}) - H(P_Y) + H(Q_Y) - H(Q_{Y_\theta})| \\
&\leq (H(P_{Y|\mathbf{X}}) - H(Q_{Y|\mathbf{X}})) + \big(\mathbb{E}_{\mathbf{x}\sim Q_{\mathbf{X}}}[H(P_\theta(\cdot|\mathbf{x}))] - \mathbb{E}_{\mathbf{x}\sim P_{\mathbf{X}}}[H(P_\theta(\cdot|\mathbf{x}))]\big) + |H(P_{Y_\theta}) - H(P_Y)| + |H(Q_Y) - H(Q_{Y_\theta})| \\
&\leq (H(P_{Y|\mathbf{X}}) - H(Q_{Y|\mathbf{X}})) + \big(\mathbb{E}_{\mathbf{x}\sim Q_{\mathbf{X}}}[H(P_\theta(\cdot|\mathbf{x}))] - \mathbb{E}_{\mathbf{x}\sim P_{\mathbf{X}}}[H(P_\theta(\cdot|\mathbf{x}))]\big) + 4\big(D_{\mathrm{JS}}^{\frac{1}{4}}(P_{Y_\theta}, P_Y) + D_{\mathrm{JS}}^{\frac{1}{4}}(Q_{Y_\theta}, Q_Y)\big) \\
&\leq \underbrace{(H(P_{Y|\mathbf{X}}) - H(Q_{Y|\mathbf{X}}))}_{\text{(A)}} + \underbrace{\big(\mathbb{E}_{\mathbf{x}\sim Q_{\mathbf{X}}}[H(P_\theta(\cdot|\mathbf{x}))] - \mathbb{E}_{\mathbf{x}\sim P_{\mathbf{X}}}[H(P_\theta(\cdot|\mathbf{x}))]\big)}_{\text{(B)}} + 8\Delta^{\frac{1}{4}}, \qquad (12)
\end{aligned}
$$

where $\Delta := \delta_P + \delta_Q$. Now, we will derive the upper-bounds for the terms (A) and (B), independently. First, by adopting Lemma E.4, we can express the term $H(P_{Y|\mathbf{X}})$ as below.

$$
\begin{aligned}
&H(P_{Y|\mathbf{X}}) \\
&= \mathbb{E}_{P_\mathbf{X}}[H(P_{Y|\mathbf{X}=\mathbf{x}}) - H(Q_{Y|\mathbf{X}=\mathbf{x}})] + \mathbb{E}_{P_\mathbf{X}}[H(Q_{Y|\mathbf{X}=\mathbf{x}})] \\
&\leq \mathbb{E}_{P_\mathbf{X}}[\big|H(P_{Y|\mathbf{X}=\mathbf{x}}) - H(Q_{Y|\mathbf{X}=\mathbf{x}})\big|] + \mathbb{E}_{P_\mathbf{X}}[H(Q_{Y|\mathbf{X}=\mathbf{x}})] \\
&\leq 4\mathbb{E}_{P_\mathbf{X}}[D_{\mathrm{JS}}^{\frac{1}{4}}(P_{Y|\mathbf{X}=\mathbf{x}}||Q_{Y|\mathbf{X}=\mathbf{x}})] + \mathbb{E}_{P_\mathbf{X}}[H(Q_{Y|\mathbf{X}=\mathbf{x}})] \\
&\leq 4\mathbb{E}_{P_\mathbf{X}}[D_{\mathrm{JS}}^{\frac{1}{4}}(P_{Y|\mathbf{X}=\mathbf{x}}||Q_{Y|\mathbf{X}=\mathbf{x}})] + \mathbb{E}_{P_\mathbf{X}}[H(Q_{Y|\mathbf{X}=\mathbf{x}})] - \mathbb{E}_{Q_\mathbf{X}}[H(Q_{Y|\mathbf{X}=\mathbf{x}})] + \mathbb{E}_{Q_\mathbf{X}}[H(Q_{Y|\mathbf{X}=\mathbf{x}})]
\end{aligned}
$$

Then, the term (A) of ineq. 12, i.e., $H(P_{Y|\mathbf{X}}) - H(Q_{Y|\mathbf{X}})$, is represented as below:

$$
H(P_{Y|\mathbf{X}}) - H(Q_{Y|\mathbf{X}}) \leq 4\mathbb{E}_{P_\mathbf{X}}[D_{\mathrm{JS}}^{\frac{1}{4}}(P_{Y|\mathbf{X}=\mathbf{x}}||Q_{Y|\mathbf{X}=\mathbf{x}})] + \mathbb{E}_{P_\mathbf{X}}[H(Q_{Y|\mathbf{X}=\mathbf{x}})] - \mathbb{E}_{Q_\mathbf{X}}[H(Q_{Y|\mathbf{X}=\mathbf{x}})]
$$

To replace $\mathbb{E}_{P_\mathbf{X}}[H(Q_{Y|\mathbf{X}=\mathbf{x}})] - \mathbb{E}_{Q_\mathbf{X}}[H(Q_{Y|\mathbf{X}=\mathbf{x}})]$ into a more interpretable term, and we start from the restatement of Lemma 1 of Shui et al. (2022).

**Lemma E.9 (restatement of Lemma 1 of Shui et al. (2022))** *Let $Z \in \mathcal{Z}$ be the real-valued integrable random variable, and denoting two distributions on a common space $\mathcal{Z}$ by $P$ and $Q$ such that $Q$ is absolutely continuous w.r.t. $P$. If for any function $f$ and $\lambda \in \mathbb{R}$ such that $\mathbb{E}_P[\exp(\lambda(f(z) - \mathbb{E}_P(f(z))))] < \infty$, then we have:*

$$
\begin{aligned}
\lambda(\mathbb{E}_Q f(z) - \mathbb{E}_P f(z)) \leq\ & D_{\mathrm{KL}}(Q||P) \\
& + \log \mathbb{E}_P[\exp(\lambda(f(z) - \mathbb{E}_P(f(z))))]
\end{aligned}
$$

Now, let $\mathbf{X}$ and $Y$ denote observable variables from a joint distribution $D_{\mathbf{X}Y} \in \{P_{\mathbf{X}Y}, Q_{\mathbf{X}Y}\}$, and we denote $f(\mathbf{x}) := H(Q_{Y|\mathbf{X}=\mathbf{x}}) \geq 0$ as a loss function of our interest, e.g., conditional entropy of $y$ given $\mathbf{x}$. Then, $f$ has a finite value of $\mathbb{E}_D[\exp(\lambda(f(\mathbf{x}) - \mathbb{E}_D(f(\mathbf{x}))))]$, and is bounded within interval $[0, \hat{H}(Q_{Y|\mathbf{x}})]$ where $\hat{H}(Q_{Y|\mathbf{x}}) := \max_{\mathbf{x}\in\mathcal{X}} H(Q_{Y|\mathbf{X}=\mathbf{x}})$.

We next define a mixture distribution $M_{\mathbf{X}Y} = \frac{1}{2}(P_{\mathbf{X}Y} + Q_{\mathbf{X}Y})$ where the support of $M_{\mathbf{X}Y}$ covers that of $P_{\mathbf{X}Y}$ and $Q_{\mathbf{X}Y}$. Then, we get the inequality below by setting $P = M_{\mathbf{X}Y}$ and $Q = Q_{\mathbf{X}Y}$ for all $\lambda > 0$ according to the Lemma E.9:

$$
\begin{aligned}
&\mathbb{E}_{Q_\mathbf{X}}[H(Q_{Y|\mathbf{X}=\mathbf{x}})] - \mathbb{E}_{M_\mathbf{X}}[H(Q_{Y|\mathbf{X}=\mathbf{x}})] \\
&\leq \frac{1}{\lambda}(\log \mathbb{E}_{M_\mathbf{X}}[\exp(\lambda(f(\mathbf{x}) - \mathbb{E}_{M_\mathbf{X}}(f(\mathbf{x}))))] + D_{\mathrm{KL}}(Q_\mathbf{X}||M_\mathbf{X})).
\end{aligned} \tag{13}
$$

Also, we get similar inequality by setting $P = M_{\mathbf{X}Y}$ and $Q = P_{\mathbf{X}Y}$ for all $\lambda < 0$ according to the Lemma E.9 as below:

$$
\begin{aligned}
&\mathbb{E}_{P_\mathbf{X}}[H(Q_{Y|\mathbf{X}=\mathbf{x}})] - \mathbb{E}_{M_\mathbf{X}}[H(Q_{Y|\mathbf{X}=\mathbf{x}})] \\
&\geq \frac{1}{\lambda}(\log \mathbb{E}_{M_\mathbf{X}}[\exp(\lambda(f(\mathbf{x}) - \mathbb{E}_{M_\mathbf{X}}(f(\mathbf{x}))))] + D_{\mathrm{KL}}(P_\mathbf{X}||M_\mathbf{X})).
\end{aligned} \tag{14}
$$

Meanwhile, give that $f(\mathbf{x})$ is bounded within interval $\hat{H}(Q_{Y|\mathbf{x}})$, the $f(\mathbf{x}) - \mathbb{E}_{M_\mathbf{X}} f(\mathbf{x})$ becomes a sub-Gaussian Wainwright (2019) with the scale parameter $\sigma = \hat{H}(Q_{Y|\mathbf{x}})/2$ at most. Then, we can leverage the property of sub-Gaussian for the log moment generating function,

$$
\log \mathbb{E}_{M_\mathbf{X}}[\exp(\lambda(f(\mathbf{x}) - \mathbb{E}_{M_\mathbf{X}}(f(\mathbf{x}))))] \leq \log(\exp(\frac{\lambda^2\sigma^2}{2})) \leq \frac{\lambda^2 \hat{H}(Q_{Y|\mathbf{x}})^2}{8}. \tag{15}
$$

By plugging the ineq. 15 into ineq. 13 and ineq. 14, we can derive the following new inequalities:

$$
\begin{aligned}
\mathbb{E}_{Q_\mathbf{X}}[H(Q_{Y|\mathbf{X}=\mathbf{x}})] - \mathbb{E}_{M_\mathbf{X}}[H(Q_{Y|\mathbf{X}=\mathbf{x}})] &\leq \frac{\lambda_0 \hat{H}(Q_{Y|\mathbf{x}})^2}{8} + \frac{1}{\lambda_0} D_{\mathrm{KL}}(Q_\mathbf{X}||M_\mathbf{X}), \\
\mathbb{E}_{M_\mathbf{X}}[H(Q_{Y|\mathbf{X}=\mathbf{x}})] - \mathbb{E}_{P_\mathbf{X}}[H(Q_{Y|\mathbf{X}=\mathbf{x}})] &\leq \frac{\lambda_0 \hat{H}(Q_{Y|\mathbf{x}})^2}{8} + \frac{1}{\lambda_0} D_{\mathrm{KL}}(P_\mathbf{X}||M_\mathbf{X}).
\end{aligned}
$$

where $\lambda_0 = \lambda$ stands for $\lambda > 0$ in the ineq. 13 and $\lambda_0 = -\lambda$ for $\lambda < 0$ in the ineq. 14.

By adding both inequalities above, and setting the $\lambda_0 = \frac{2}{\hat{H}(Q_{Y|\mathbf{x}})}\sqrt{D_{\mathrm{KL}}(P_{\mathbf{X}}||M_{\mathbf{X}}) + D_{\mathrm{KL}}(Q_{\mathbf{X}}||M_{\mathbf{X}})}$ results in:

$$\mathbb{E}_{Q_{\mathbf{X}}}[H(Q_{Y|\mathbf{X}=\mathbf{x}})] - \mathbb{E}_{P_{\mathbf{X}}}[H(Q_{Y|\mathbf{X}=\mathbf{x}})] \leq \hat{H}(Q_{Y|\mathbf{x}})\sqrt{2D_{\mathrm{JS}}(P_{\mathbf{X}}||Q_{\mathbf{X}})}. \tag{16}$$

Next, a decomposition of KL divergence and the definition of JS divergence leads to the following inequality,

$$\begin{aligned}
&= 2D_{\mathrm{JS}}(P_{X_v X_t}||Q_{X_v X_t}) \\
&= D_{\mathrm{KL}}(P_{X_v X_t}||M_{X_v X_t}) + D_{\mathrm{KL}}(Q_{X_v X_t}||M_{X_v X_t}) \\
&= \frac{1}{2}\big(D_{\mathrm{KL}}(P_{X_v}||M_{X_v}) + \mathbb{E}_{P_{X_v}} D_{\mathrm{KL}}(P_{X_t|X_v=x_v}||M_{X_t|X_v=x_v})\big) + \frac{1}{2}\big(D_{\mathrm{KL}}(Q_{X_v}||M_{X_v}) + \mathbb{E}_{Q_{X_v}} D_{\mathrm{KL}}(Q_{X_t|X_v=x_v}||M_{X_t|X_v=x_v})\big) \\
&+ \frac{1}{2}\big(D_{\mathrm{KL}}(P_{X_t}||M_{X_t}) + \mathbb{E}_{P_{X_t}} D_{\mathrm{KL}}(P_{X_v|X_t=x_t}||M_{X_v|X_t=x_t})\big) + \frac{1}{2}\big(D_{\mathrm{KL}}(Q_{X_t}||P_{X_t}) + \mathbb{E}_{Q_{X_t}} D_{\mathrm{KL}}(Q_{X_v|X_t=x_t}||M_{X_v|X_t=x_t})\big) \\
&= D_{\mathrm{JS}}(P_{X_v}||Q_{X_v}) + D_{\mathrm{JS}}(P_{X_t}||Q_{X_t}) \\
&+ \frac{1}{2}\big(\mathbb{E}_{P_{X_v}} D_{\mathrm{KL}}(P_{X_t|X_v=x_v}||M_{X_t|X_v=x_v}) + \mathbb{E}_{Q_{X_v}} D_{\mathrm{KL}}(Q_{X_t|X_v=x_v}||M_{X_t|X_v=x_v})\big) \\
&+ \frac{1}{2}\big(\mathbb{E}_{P_{X_t}} D_{\mathrm{KL}}(P_{X_v|X_t=x_t}||M_{X_v|X_t=x_t}) + \mathbb{E}_{Q_{X_t}} D_{\mathrm{KL}}(Q_{X_v|X_t=x_t}||M_{X_v|X_t=x_t})\big) \\
&\leq D_{\mathrm{JS}}(P_{X_v}||Q_{X_v}) + D_{\mathrm{JS}}(P_{X_t}||Q_{X_t}) + \bar{D}_{\mathrm{JS}}(P_{X_t|X_v}||Q_{X_t|X_v}) + \bar{D}_{\mathrm{JS}}(P_{X_v|X_t}||Q_{X_v|X_t})
\end{aligned}$$

where $\bar{D}_{\mathrm{JS}}(P_{Y|X}||Q_{Y|X}) := \mathbb{E}_{x\sim P_X} D_{\mathrm{JS}}(P_{Y|X=x}||Q_{Y|X=x}) + \mathbb{E}_{x\sim Q_X} D_{\mathrm{JS}}(P_{Y|X=x}||Q_{Y|X=x})$

Based on the above decomposition, we can modify the bound as below,

$$\begin{aligned}
&\mathbb{E}_{Q_{\mathbf{X}}}[H(Q_{Y|\mathbf{X}=\mathbf{x}})] - \mathbb{E}_{P_{\mathbf{X}}}[H(Q_{Y|\mathbf{X}=\mathbf{x}})] \\
&\leq \hat{H}(Q_{Y|\mathbf{x}})\sqrt{2D_{\mathrm{JS}}(P_{\mathbf{X}}||Q_{\mathbf{X}})} \\
&\leq \hat{H}(Q_{Y|\mathbf{x}})\sqrt{D_{\mathrm{JS}}(P_{X_v}||Q_{X_v}) + D_{\mathrm{JS}}(P_{X_t}||Q_{X_t}) + \bar{D}_{\mathrm{JS}}(P_{X_t|X_v}||Q_{X_t|X_v}) + \bar{D}_{\mathrm{JS}}(P_{X_v|X_t}||Q_{X_v|X_t})}.
\end{aligned}$$

Therefore, we get an upper-bound for the (A) term in ineq. 12 as below,

$$\begin{aligned}
H(P_{Y|\mathbf{X}}) - H(Q_{Y|\mathbf{X}}) &\leq H(Q_Y)\sqrt{D_{\mathrm{JS}}(P_{X_v}||Q_{X_v}) + D_{\mathrm{JS}}(P_{X_t}||Q_{X_t}) + \bar{D}_{\mathrm{JS}}(P_{X_t|X_v}||Q_{X_t|X_v}) + \bar{D}_{\mathrm{JS}}(P_{X_v|X_t}||Q_{X_v|X_t})} \\
&\quad + 4\mathbb{E}_{P_{\mathbf{X}}}[D^{\frac{1}{4}}_{\mathrm{JS}}(P_{Y|\mathbf{X}=\mathbf{x}}||Q_{Y|\mathbf{X}=\mathbf{x}})] \\
&\leq \hat{H}(Q_{Y|\mathbf{x}})\big(D^{\frac{1}{2}}_{\mathrm{JS}}(P_{X_v}||Q_{X_v}) + D^{\frac{1}{2}}_{\mathrm{JS}}(P_{X_t}||Q_{X_t})\big) \\
&\quad + \hat{H}(Q_{Y|\mathbf{x}})\big(\bar{D}^{\frac{1}{2}}_{\mathrm{JS}}(P_{X_t|X_v}||Q_{X_t|X_v}) + \bar{D}^{\frac{1}{2}}_{\mathrm{JS}}(P_{X_v|X_t}||Q_{X_v|X_t})\big) \\
&\quad + 4\mathbb{E}_{P_{\mathbf{X}}}[D^{\frac{1}{4}}_{\mathrm{JS}}(P_{Y|\mathbf{X}=\mathbf{x}}||Q_{Y|\mathbf{X}=\mathbf{x}})].
\end{aligned}$$

Then, deriving a bound for the remaining (B) term in ineq. 12, i.e., $\mathbb{E}_{\mathbf{x}\sim Q_{\mathbf{X}}}[H(P_\theta(\cdot|\mathbf{x}))] - \mathbb{E}_{\mathbf{x}\sim P_{\mathbf{X}}}[H(P_\theta(\cdot|\mathbf{x}))]$, is very similar to the procedure of deriving the upper-bound for the term (A) by switching $Q_{Y|\mathbf{X}}$ to $P_\theta(\cdot|\mathbf{X})$ and set the $f$ for Lemma E.9 as $f(\mathbf{x}) := H(P_\theta(\cdot|\mathbf{x}))$, thereby having the interval $[0, \hat{H}(P_\theta)]$ where $\hat{H}(P_\theta) : \max_{\mathbf{x}\in\mathcal{X}} H(P_\theta(\cdot|\mathbf{x}))$. This induces an upper-bound as below,

$$\begin{aligned}
&\mathbb{E}_{\mathbf{x}\sim Q_{\mathbf{X}}}[H(P_\theta(\cdot|\mathbf{x}))] - \mathbb{E}_{\mathbf{x}\sim P_{\mathbf{X}}}[H(P_\theta(\cdot|\mathbf{x}))] \\
&\leq \hat{H}(P_\theta)\sqrt{2D_{\mathrm{JS}}(P_{\mathbf{X}}||Q_{\mathbf{X}})} \\
&\leq \hat{H}(P_\theta)\big(D^{\frac{1}{2}}_{\mathrm{JS}}(P_{X_v}||Q_{X_v}) + D^{\frac{1}{2}}_{\mathrm{JS}}(P_{X_t}||Q_{X_t}) + \bar{D}^{\frac{1}{2}}_{\mathrm{JS}}(P_{X_t|X_v}||Q_{X_t|X_v}) + \bar{D}^{\frac{1}{2}}_{\mathrm{JS}}(P_{X_v|X_t}||Q_{X_v|X_t})\big).
\end{aligned} \tag{17}$$

Finally, we complete the proof by adding the ineq. E.2 and ineq. 17 to induces the upper bound of $\mathrm{EMID}(P_{\mathbf{X}Y}, Q_{\mathbf{X}Y}; \theta)$,

$$
\begin{aligned}
&\text{EMID}(P_{\mathbf{X}Y}, Q_{\mathbf{X}Y}; \theta) \\
&\leq (H(P_{Y|\mathbf{X}}) - H(Q_{Y|\mathbf{X}})) + \big(\mathbb{E}_{\mathbf{x}\sim Q_{\mathbf{X}}}[H(P_\theta(\cdot|\mathbf{x}))] - \mathbb{E}_{\mathbf{x}\sim P_{\mathbf{X}}}[H(P_\theta(\cdot|\mathbf{x}))]\big) + 8\Delta^{\frac{1}{4}} \\
&\leq \hat{H}\big(D_{\mathrm{JS}}^{\frac{1}{2}}(P_{X_v}||Q_{X_v}) + D_{\mathrm{JS}}^{\frac{1}{2}}(P_{X_t}||Q_{X_t})\big) \\
&+ \hat{H}\big(\bar{D}_{\mathrm{JS}}^{\frac{1}{2}}(P_{X_t|X_v}||Q_{X_t|X_v}) + \bar{D}_{\mathrm{JS}}^{\frac{1}{2}}(P_{X_v|X_t}||Q_{X_v|X_t})\big) \\
&+ 4\mathbb{E}_{P_{\mathbf{X}}}[D_{\mathrm{JS}}^{\frac{1}{4}}(P_{Y|\mathbf{X}=\mathbf{x}}||Q_{Y|\mathbf{X}=\mathbf{x}})] + 8\Delta^{\frac{1}{4}}
\end{aligned}
$$

where $\widehat{H} = \max_{\mathbf{x}\in\mathcal{X}}[H(Q_{Y|\mathbf{X}=\mathbf{x}}) + H(P_\theta(\cdot|\mathbf{x}))]$ and $\Delta = \delta_P + \delta_Q$.

Then, we introduce an assumption over the consistency between conditional distributions as below.

**Assumption E.10 (Consistency of conditional distributions)** *For the distributions $P_{\mathbf{X}Y}$ and $Q_{\mathbf{X}Y}$ over $\mathcal{X}\times\mathcal{Y}$, conditional distributions of $X_t$ given $X_v$, $X_v$ given $X_t$, and $Y$ given $\mathbf{X} = (X_v, X_t)$ are consistent between $P_{\mathbf{X}}Y$ and $Q_{\mathbf{X}}Y$. That is,*

- $P_{X_t|X_v} = Q_{X_t|X_v}$ *and* $P_{X_v|X_t} = Q_{X_v|X_t}$,
- $P_{Y|\mathbf{X}} = Q_{Y|\mathbf{X}}$.

Finally, we present the simplified version of EMID upper bound by leveraging the Assumption E.10.

**Theorem E.11 (Simplified scenario)** *Given an MLLM $P_\theta$ and distributions $P_{\mathbf{X}Y}$, $Q_{\mathbf{X}Y}$ which have consistent conditional distributions over variables $X_v|X_t$, $X_t|X_v$, and $Y|\mathbf{X}$, if there exist some constants $\delta_P$ and $\delta_Q$ such that*

$$D_{\mathrm{JS}}(P_{Y_\theta}\|P_Y) \leq \delta_P, \quad D_{\mathrm{JS}}(Q_{Y_\theta}\|Q_Y) \leq \delta_Q,$$

*where $P_{Y_\theta} = \mathbb{E}_{\mathbf{x}\sim P_{\mathbf{X}}} P_\theta(\cdot|\mathbf{x})$ and $Q_{Y_\theta} = \mathbb{E}_{\mathbf{x}\sim Q_{\mathbf{X}}} P_\theta(\cdot|\mathbf{x})$, then EMID$(P_{\mathbf{X}Y}, Q_{\mathbf{X}Y}; \theta)$ is upper bounded by*

$$\widehat{H}\big(D_{\mathrm{JS}}^{\frac{1}{2}}(P_{X_v}\|Q_{X_v}) + D_{\mathrm{JS}}^{\frac{1}{2}}(P_{X_t}\|Q_{X_t})\big) + 8\Delta^{\frac{1}{4}}, \tag{18}$$

*where $\widehat{H} = \max_{\mathbf{x}\in\mathcal{X}}[H(Q_{Y|\mathbf{X}=\mathbf{x}}) + H(P_\theta(\cdot|\mathbf{x}))]$ and $\Delta = \delta_P + \delta_Q$.*

Given Theorem E.8, Assumption E.10 zeros out the terms $\big(\bar{D}_{\mathrm{JS}}^{\frac{1}{2}}(P_{X_t|X_v}\|Q_{X_t|X_v}) + \bar{D}_{\mathrm{JS}}^{\frac{1}{2}}(P_{X_v|X_t}\|Q_{X_v|X_t})\big)$ and $\mathbb{E}_{\mathbf{x}\sim P_{\mathbf{X}}}[D_{\mathrm{JS}}^{\frac{1}{4}}(P_{Y|\mathbf{X}=\mathbf{x}}\|Q_{Y|\mathbf{X}=\mathbf{x}})]$ which induces Eq. 18, accordingly.

**Corollary E.12** *Given an MLLM $P_\theta$ and distributions $P_{\mathbf{X}Y}$, $Q_{\mathbf{X}Y}$ which have consistent conditional distributions over variables $X_v|X_t$, $X_t|X_v$, and $Y|\mathbf{X}$, EMID$(P_{\mathbf{X}Y}, Q_{\mathbf{X}Y}; \theta)$ is upper bounded by*

$$
\begin{aligned}
&\widehat{H}\big(D_{\mathrm{JS}}^{\frac{1}{2}}(P_{X_v}\|Q_{X_v}) + D_{\mathrm{JS}}^{\frac{1}{2}}(P_{X_t}\|Q_{X_t})\big) \\
&+ 8(\mathbb{E}_{\mathbf{x}\sim P_{\mathbf{X}}} D_{\mathrm{TV}}(P_{Y|\mathbf{X}=\mathbf{x}}, P_\theta(\cdot|\mathbf{x})) + \mathbb{E}_{\mathbf{x}\sim Q_{\mathbf{X}}} D_{\mathrm{TV}}(Q_{Y|\mathbf{X}=\mathbf{x}}, P_\theta(\cdot|\mathbf{x})))^{\frac{1}{4}},
\end{aligned}
\tag{19}
$$

*where $D_{\mathrm{TV}}(\cdot,\cdot)$ is the total variation distance, and $\widehat{H} = \max_{\mathbf{x}\in\mathcal{X}}[H(Q_{Y|\mathbf{X}=\mathbf{x}}) + H(P_\theta(\cdot|\mathbf{x}))]$.*

Let $P_{Y_\theta} = \mathbb{E}_{\mathbf{x}\sim P_{\mathbf{X}}} P_\theta(\cdot|\mathbf{x})$ and $Q_{Y_\theta} = \mathbb{E}_{\mathbf{x}\sim Q_{\mathbf{X}}} P_\theta(\cdot|\mathbf{x})$, then $D_{\mathrm{JS}}(\cdot|\cdot) \leq D_{\mathrm{TV}}(\cdot,\cdot)$ allow us to induce below,

$$
\begin{aligned}
D_{\mathrm{JS}}(P_{Y_\theta}\|P_Y) &= \mathbb{E}_{\mathbf{x}\sim P_{\mathbf{X}}}[D_{\mathrm{JS}}(P_\theta(\cdot|\mathbf{x})\|P_{Y|\mathbf{X}=\mathbf{x}})] \leq \mathbb{E}_{\mathbf{x}\sim P_{\mathbf{X}}}[D_{\mathrm{TV}}(P_{Y|\mathbf{X}=\mathbf{x}}, P_\theta(\cdot|\mathbf{x}))], \\
D_{\mathrm{JS}}(Q_{Y_\theta}\|Q_Y) &= \mathbb{E}_{\mathbf{x}\sim Q_{\mathbf{X}}}[D_{\mathrm{JS}}(P_\theta(\cdot|\mathbf{x})\|Q_{Y|\mathbf{X}=\mathbf{x}})] \leq \mathbb{E}_{\mathbf{x}\sim Q_{\mathbf{X}}}[D_{\mathrm{TV}}(Q_{Y|\mathbf{X}=\mathbf{x}}, P_\theta(\cdot|\mathbf{x}))].
\end{aligned}
\tag{20}
$$

Noting that $a^{\frac{1}{4}} + b^{\frac{1}{4}} \leq 2(a+b)^{\frac{1}{4}}$ for $a, b \geq 0$, plugging the above inequality into the Theorem E.11 complete the proof. Although this alternative upper bound is looser than Theorem E.11, Corollary E.12 is more interpretable in the sense that it directly represents the model-specific discrepancy terms via distance between model output distribution and true conditional distributions, rather than expresses it through marginal distribution terms in $D_{\mathrm{JS}}(P_{Y_\theta}||P_Y)$ and $D_{\mathrm{JS}}(Q_{Y_\theta}||Q_Y)$. Therefore, as our model becomes more accurate at modeling the ground truth conditional distribution of $Y$ given $\mathbf{X}$, the EMID mainly depends on the divergence between the marginal distributions of visual and text inputs.